

1 **Pesticide-induced resurgence of the brown planthopper is mediated by**
2 **diverse actors that promote juvenile hormone biosynthesis and female**
3 **fecundity**

4 Yang Gao^{a*}, Shao-Cong Su^{a*}, Zhao-Yu Liu^a, Dick R. Nässel^b, Chris Bass^c,
5 Cong-Fen Gao^a, Shun-Fan Wu^{a,*}

6 ^a College of Plant Protection, Nanjing Agricultural University, Nanjing
7 210095, China.

8 ^b Department of Zoology, Stockholm University, Stockholm, Sweden

9 ^c College of Life and Environmental Sciences, Biosciences, University of
10 Exeter, Penryn Campus, Penryn, UK

11 * These authors contributed equally to this work.

12 *Corresponding author. E-mail address: wusf@njau.edu.cn (S.-F. Wu)

13 **Abstract**

14 Pesticide-induced resurgence, increases in pest insect populations following
15 pesticide application, is a serious threat to the sustainable control of many highly
16 damaging crop pests. Resurgence can result from pesticide-enhanced pest
17 reproduction, however, the molecular mechanisms mediating this process remain
18 unresolved. Here we show that brown planthopper (BPH) resurgence following
19 emamectin benzoate (EB) exposure results from the coordinated action of a diverse
20 suite of actors that regulate juvenile hormone (JH) levels, resulting in increased JH
21 titer in adult females and enhanced fecundity. Following reports of BPH resurgence in
22 rice crops when this species is exposed to EB, we demonstrate that EB treatment
23 results in profound changes in female BPH fitness including enhanced ovary
24 development and elevated egg production. This enhanced reproductive fitness
25 results from the EB-mediated upregulation of key genes involved in the regulation of
26 JH, including *JHAMT*, *Met* and *Kr-h1* and the downregulation of allatostatin (*AstA*)
27 and allatostatin receptor (*AstAR*) expression. The remodulation of gene expression
28 following EB exposure is dependent on the action of this insecticide on its molecular
29 target the glutamate-gated chloride channel (GluCl) receptor. Collectively, these
30 results provide mechanistic insights into the regulation of negative pesticide-induced
31 responses in insects and reveal the key actors involved in the JH-signaling pathway
32 that underpin pesticide resurgence.

33

34 Introduction

35 Chemical pesticides remain the primary means of controlling many of the world's
36 most damaging arthropod crop pests [1, 2]. However, pesticide applications can result
37 in pest resurgence, increases in pest insect populations that exceed natural, untreated
38 population sizes, following an initial reduction of the pest population [3-5]. Two
39 mechanisms have been implicated in pest resurgence - the loss of beneficial insects
40 including natural enemies and pesticide-enhanced pest reproduction [3]. In the case
41 of the latter, several pesticides, such as the insecticides triazophos, deltamethrin and
42 the fungicide jinggangmycin, have been reported to stimulate pest reproduction [6-8].
43 Pesticide-enhanced pest reproduction has been linked to changes in physiology and
44 biochemistry of pest organisms after exposure to pesticides [3, 4]. However, the
45 molecular mechanisms underlying enhanced reproduction associated with pest
46 resurgence remain poorly resolved.

47 The brown planthopper (BPH), *Nilaparvata lugens* (Stål), is a notorious pest of
48 rice crops throughout Asia causing annual losses of ~300 million dollars across major
49 rice producing countries [2, 3]. BPH inhibits the growth of rice plants by feeding, and
50 also transmits highly damaging plant viruses including rice grassy stunt virus and rice
51 ragged stunt virus [9]. Currently, chemical insecticides play an indispensable role in
52 the control of BPH due to their efficiency, rapid effect, and low cost. However, due to
53 the widespread and intensive use of chemical insecticides, BPH has developed
54 resistance to the majority of compounds used for control [2, 10].

55 Emamectin benzoate (EB) and abamectin are avermectin pesticides, and act as

56 allosteric modulators of insect glutamate gated chloride channels (GluCl_s), inhibiting
57 muscle contractions that lead to the cessation of insect feeding and subsequent death
58 [11]. These insecticides exhibit particularly strong activity against Lepidoptera such as
59 the rice leaffolder, *Cnaphalocrocis medinalis* Guénee, an important foliage-feeding
60 insect which attacks rice during the vegetative stage [12]. Both BPH and the rice
61 leaffolder are migratory pests with overlapping migratory paths, however, their
62 occurrence period in the field differs by approximately one month, with leaffolders
63 appearing earlier than BPH. Therefore, the use of EB to control rice leaffolder has the
64 potential to impact BPH arriving later, via exposure to sublethal concentrations of this
65 compound. In this regard, we have observed that when farmers use EB and abamectin
66 to control leaffolders on rice crops in China, BPH outbreaks frequently occur in the
67 same field. While sublethal doses of certain pesticides have been shown to enhance
68 fecundity in BPH, including the insecticides triazophos and deltamethrin [6, 7, 13, 14]
69 and the fungicides carbendazim and jinggangmycin [8], whether avermectins trigger
70 resurgence in BPH via insecticide-enhanced reproduction remains unclear.

71 Reproduction in insects is influenced by external factors such as light [15],
72 temperature [16], humidity [17] and nutrition [18], and endogenous factors such as the
73 juvenile hormone (JH) [19], ecdysone [20], insulin [21] and TOR [22] pathways [23, 24].
74 Of these, JH, has been particularly implicated in insecticide-induced enhanced
75 fecundity, with triazophos and deltamethrin treatments leading to increased circulating
76 JH III titers in BPH females [3]. JH is synthesized and secreted by the corpora allata
77 in insects [25], and can promote reproduction by regulating the synthesis and secretion

78 of vitellogenin (vg) in the female fat body, and stimulating the absorption of vg by the
79 developing oocyte [19]. However, the regulation of JH is complex [19] and the key
80 actors involved in JH-mediated pesticide-enhanced reproduction remains an open
81 question.

82 In this study, we used a diverse range of approaches to investigate the impact of
83 sublethal doses of avermectins on BPH fecundity, and unravel the molecular
84 mechanisms mediating enhanced reproduction following exposure to this insecticide
85 class. We show that avermectin exposure results in profound changes in the
86 expression of a key suite of genes that in combination regulate JH, resulting in
87 increased JH titer in adult females, which promotes fecundity.

88

89 **RESULTS**

90 **GluCl allosteric modulators (emamectin benzoate and abamectin) stimulate**
91 **fecundity of female *N. lugens***

92 To investigate whether GluCl modulators affect fecundity in BPH, we first
93 determined the sub-lethal and median lethal doses of emamectin benzoate (EB) to
94 4th instar nymphs, newly emerged males and females of BPH ([Table S1](#)). For this we
95 employed two different bioassay methods, the rice seedling dip bioassay method and
96 topical application bioassay method [[2](#), [26](#)], in order to assess both the systemic and
97 contact toxicity of these insecticides ([Table S1](#)). We then systemically treated 4th
98 instar nymphs of BPH with the estimated LC₁₅ and LC₅₀ concentrations of EB and
99 examined the fecundity of BPH after these individuals mated with treated or
100 untreated individuals. We use the term “t” to represent individuals treated with EB
101 and “ck” to indicate control individuals that were treated with insecticide diluent minus
102 insecticide. After treatment with the LC₁₅ and LC₅₀ concentrations of EB the number
103 of eggs laid per female of BPH in ♀t × ♂t crosses increased by 1.48 and 1.40 times
104 compared with control ♀ck × ♂ck crosses ([Figure 1A](#)); the number of eggs laid per
105 female of BPH in ♀t × ♂ck crosses increased by 1.53 and 2.07 times compared with
106 control crosses ([Figure 1B](#)); However, the number of eggs laid by per female of BPH
107 in ♀ck × ♂t crosses did not increase significantly compared to control ♀ck × ♂ck
108 crosses ([Figure 1C](#)).

Table S1. Determination of the toxicity of emamectin benzoate against BPH in systemic and topical application bioassays.

Treatment method	Developmental stages	Slope \pm SE	LC ₁₅ (95%F.L.)	LC ₅₀ (95%F.L.)	χ^2 (df)	<i>P</i> value
			(mg/L) or LD ₁₅ (95%F.L.) (pg/insect)	(mg/L) or LD ₅₀ (95%F.L.) (pg/insect)		
Systemic route	4 th nymph	2.56 \pm 0.487	0.87 (0.39-1.32)	2.21 (1.53- 2.82)	2.68 (4)	0.61
	Male	2.42 \pm 0.35	0.80 (0.40-1.20)	2.13 (1.48- 2.78)	2.12 (4)	0.72
	Female	2.47 \pm 0.41	2.33 (1.09-3.56)	6.12 (4.18- 8.00)	3.56 (4)	0.50
Contact route	4 th nymph	2.52 \pm 0.35	15.54 (9.46- 21.42)	39.90 (30.66- 49.56)	2.60 (4)	0.63
	Male	2.77 \pm 0.57	6.72 (2.52-10.92)	15.96 (9.66-21.84)	1.23 (3)	0.75

110

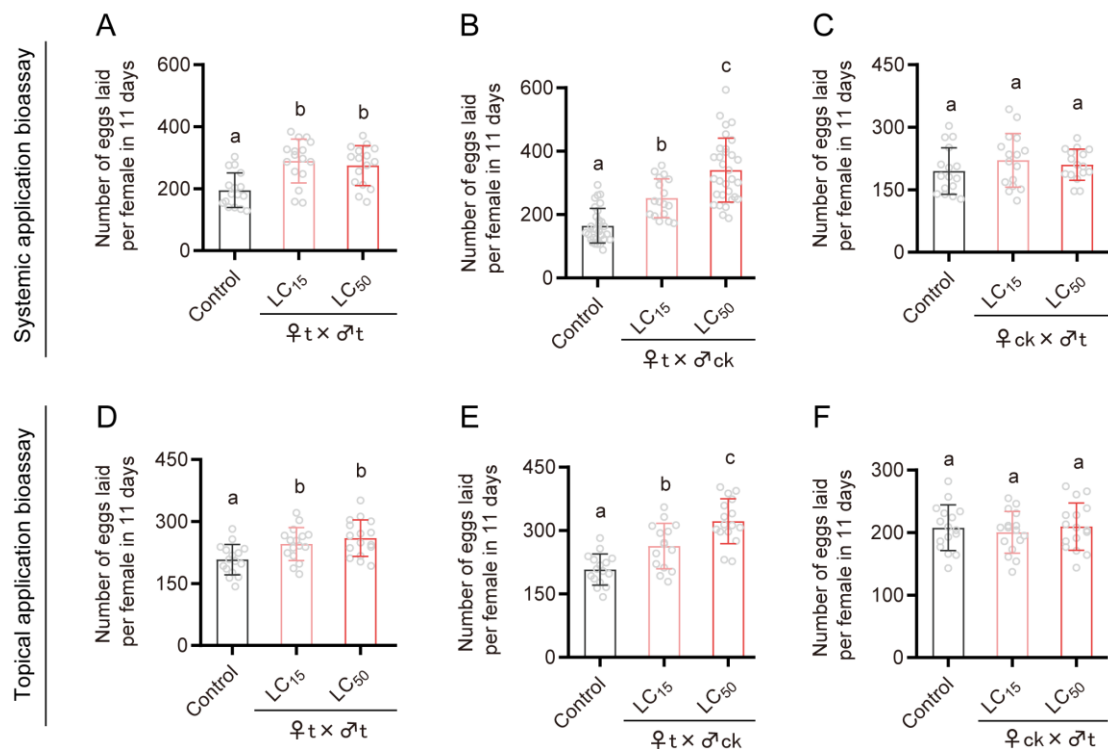
111

112

			18.48 (6.72-	37.80		
	Female	3.31 ± 0.76	28.14)	(23.10-50.40)	0.79 (3)	0.85

113 Exposure of 4th instar nymphs with the LC₁₅ and LC₅₀ concentrations of EB in
114 contact bioassays also significantly stimulated fecundity. After treatment with the LC₁₅
115 and LC₅₀ concentrations of EB, the number of eggs laid by per female of BPH in ♀t ×
116 ♂t crosses increased by 1.18 and 1.26 times compared with the control (♀ck × ♂ck)
117 (Figure 1D); The number of eggs laid per female of BPH in ♀t × ♂ck crosses
118 increased by 1.27 and 1.56 times compared with the control crosses (Figure 1E);
119 However, there was no significant difference in egg-laying number between ♀ck × ♂t
120 crosses and controls (♀ck × ♂ck) (Figure 1F). These results reveal that EB can
121 stimulate the fecundity of females following both the systemic and contact routes of
122 exposure.

123 **Figure 1**



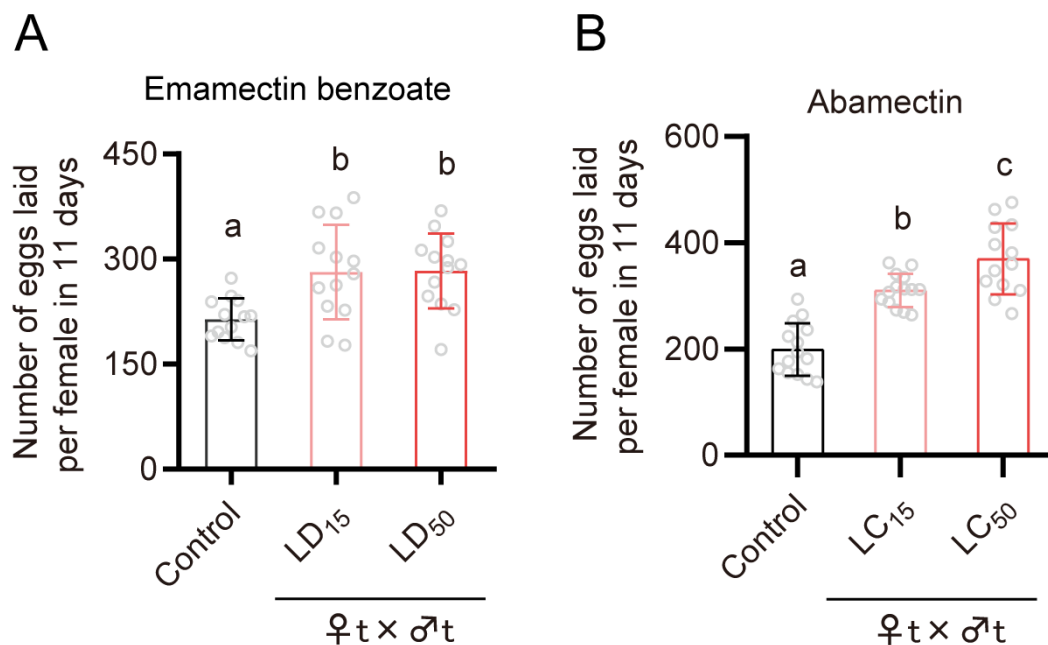
124
125 **Figure 1.** Fecundity of BPH following exposure to sub-lethal (LC₁₅) and median lethal (LC₅₀)
126 concentrations of emamectin benzoate following system application bioassays (A: ♀t × ♂t;
127 B: ♀t × ♂ck; C: ♀ck × ♂t) and topical application bioassays (D: ♀t × ♂t; E: ♀t × ♂ck; F:

128 ♀ ck × ♂ t), respectively. The letter “t” represents treatment with insecticide, while “ck”
129 indicates controls that was not treated with insecticide. All data are presented as the mean ±
130 s.e.m. Different lower-case letters above the bars indicate significant differences (One-way
131 ANOVA with Tukey’s Multiple Range Test, $p < 0.05$).

132

133 We next examined whether EB treatment of adult BPH also stimulates
134 reproduction. Indeed, treating newly emerged adults with the LC₁₅ and LC₅₀
135 concentrations of EB significantly stimulated the number of eggs laid per female
136 (Figure 1-figure supplement 1A). Furthermore, sub-lethal exposure of 4th instar BPH
137 nymphs to another GluCl allosteric modulator, abamectin (LC₁₅ and LC₅₀
138 concentrations) was also found to significantly enhance reproduction (Figure 1-figure
139 supplement 1B).

140 **Figure 1-figure supplement 1**



141

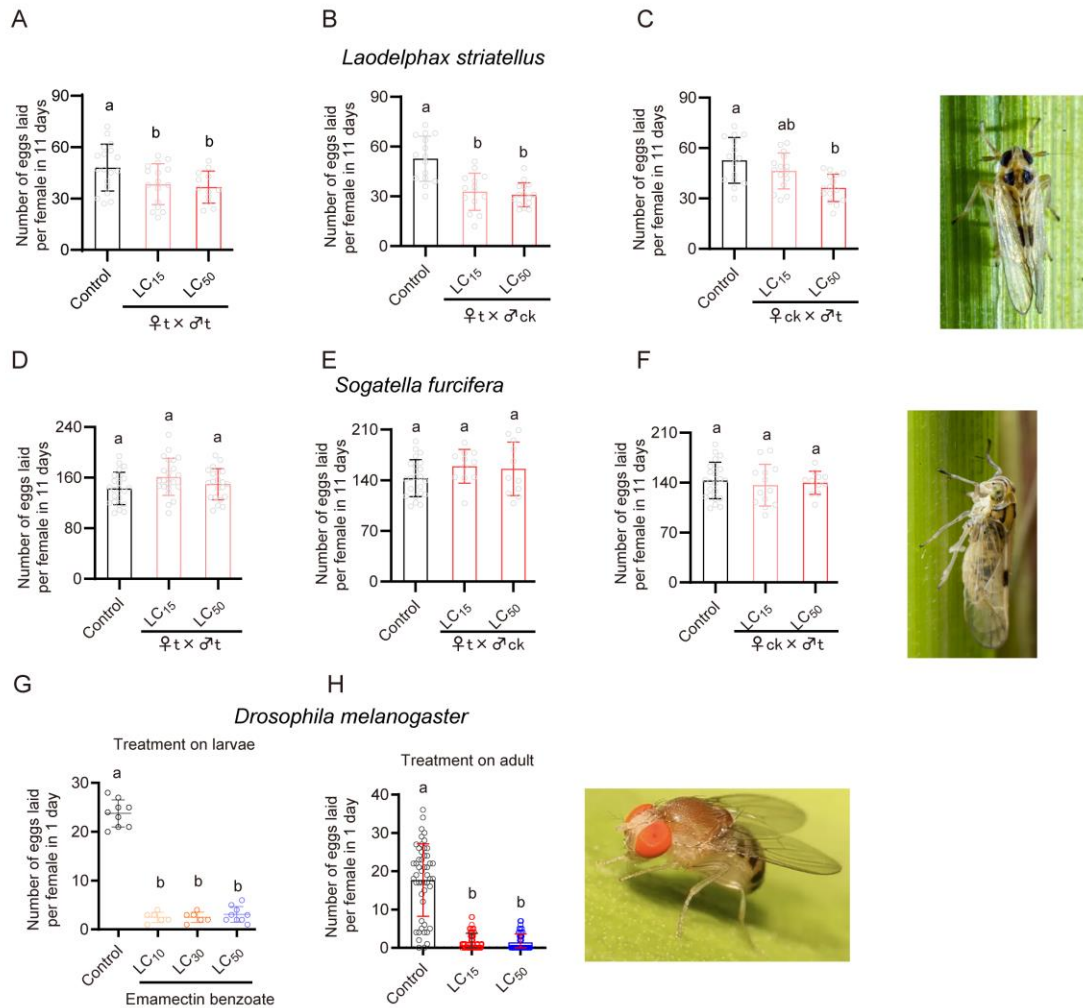
Treatment on adult Treatment on nymph

142 **Figure 1-figure supplement 1.** (A) Fecundity of BPH when newly emerged adults were
143 treated with sub-lethal (LD₁₅) and median lethal (LD₅₀) concentrations of emeactin benzoate

144 via topical application. (B) Fecundity of BPH when 4th instar nymphs were treated with sub-
145 lethal (LC₁₅) and median lethal (LC₅₀) concentrations of abamectin via systemic exposure. All
146 data are presented as the mean ± s.e.m. Different lower-case letters above the bars indicate
147 significant differences (One-way ANOVA with Tukey's Multiple Range Test, $p < 0.05$).

148 To examine if EB also stimulates egg-laying in other insect species we
149 conducted bioassays on the small brown planthopper, *Laodelphax striatellus*, the
150 white backed planthopper, *Sogatella furcifera* and fruit flies *Drosophila melanogaster*.
151 In contrast to our findings on BPH, we found that sub-lethal doses (LC₁₅ and LC₅₀) of
152 EB inhibits fecundity of female *L. striatellus*, ([Figure1-figure supplement 2A-C](#)) and
153 has no impact on the fecundity of *S. furcifera*, ([Figure1-figure supplement 2D-F](#)). In
154 addition, we found that sublethal doses (LC₁₅ or LC₅₀) of EB also inhibit fecundity in
155 *D. melanogaster* ([Figure1-figure supplement 2G and H](#)). These results indicate that
156 the stimulation of reproduction by EB in BPH is species-specific and does not extend
157 to even related insect species.

158 **Figure 1-figure supplement 2**



159

160 **Figure 1-figure supplement 2.** Fecundity of small brown planthopper, *Laodelphax striatellus*,

161 (A-C) white backed planthopper, *Sogatella furcifera* (D-F) and fruit fly, *Drosophila*

162 *melanogaster* (G and H) when larvae and newly emerged adults were treated with sub-lethal

163 concentrations of emamectin benzoate. All data are presented as the mean ± s.e.m. Different

164 lower-case letters above the bars indicate significant differences (One-way ANOVA with

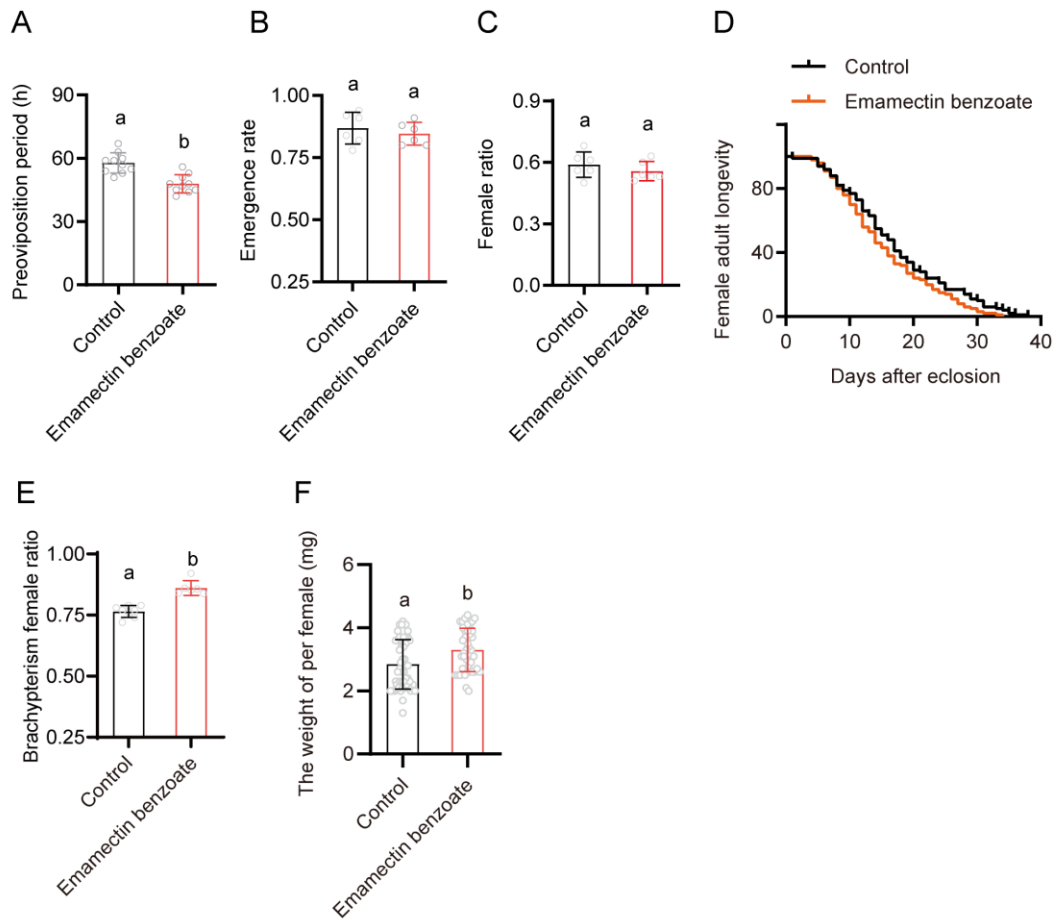
165 Tukey's Multiple Range Test, $p < 0.05$).

166

167 **The impact of EB treatment on BPH reproductive fitness**

168 To better understand the effects of EB on the reproductive fitness of BPH, the
169 preoviposition period, emergence rate, female ratio, female longevity and female
170 weight were evaluated following exposure using the systemic bioassay. The
171 preoviposition period of females treated with the LC₅₀ of EB decreased significantly
172 compared with the control ([Figure 1-figure supplement 3A](#)). In contrast no significant
173 effects of EB on emergence rate and female ratio were observed ([Figure 1-figure
174 supplement 3B and C](#)). Female survival analysis showed that exposure of 4th instar
175 nymphs to the LC₅₀ of EB has no impact on female longevity ([Figure 1-figure
176 supplement 3D](#)). Interestingly, brachypterism (long-wing) female ratio and female
177 weight were significantly increased after EB exposure ([Figure 1-figure supplement 3E
178 and F](#)).
179

180 **Figure 1-figure supplement 3**



181

182 **Figure 1-figure supplement 3.** The impact of emamectin benzoate on the reproductive

183 fitness of BPH. Fourth instar nymphs were treated with the LC₅₀ concentration of emamectin

184 benzoate in systemic bioassays. All data are presented as the mean \pm s.e.m. Different lower-

185 case letters above the bars indicate significant differences (Student's *t* test, $p < 0.05$).

186

187 **EB promotes ovarian development in BPH**

188 To investigate the cause of increased female weight following EB exposure we

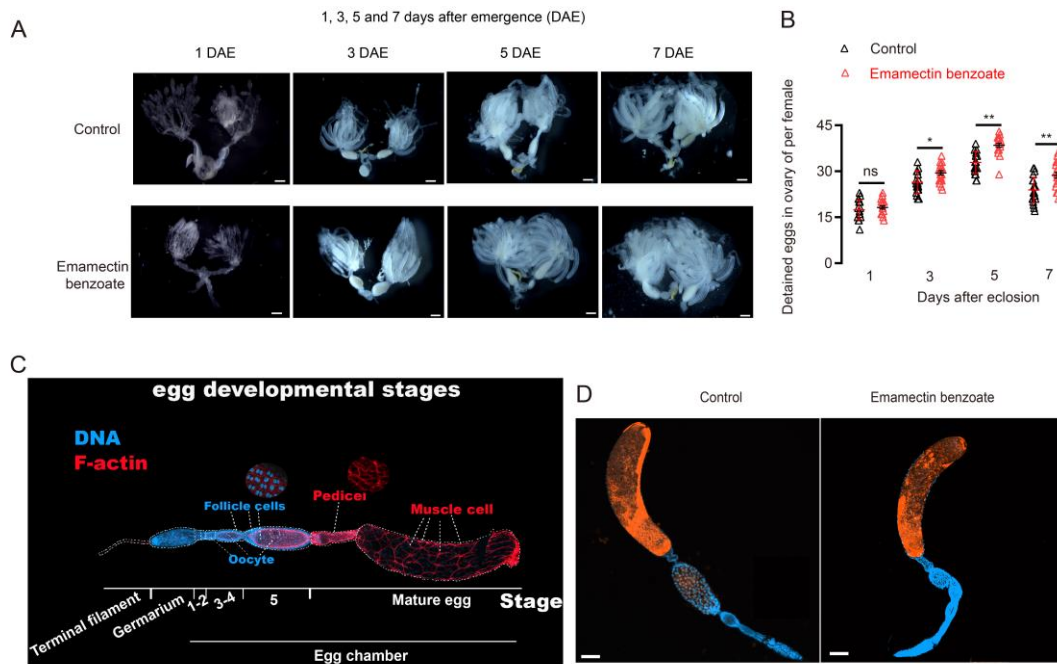
189 examined if EB influences ovary development in BPH. We dissected and compared

190 the ovaries of females treated with the LC₅₀ of EB at 1, 3, 5 and 7 days after eclosion

191 (DAE) with control females. At 3, 5 and 7 DAE, the number of detained eggs of BPH

192 in the EB treated group were significantly higher than that of controls (Figure 2A and
193 B). We also explored whether EB treatment could enhance or impair oogenesis in
194 BPH. However, dissection of various developmental stages revealed that emamectin
195 benzoate treatment has no significant effects on oogenesis (Figure 2C and D).

196 **Figure 2**



197
198 **Figure 2.** The impact of emamectin benzoate on ovary development in BPH. Fourth instar
199 nymphs were treated with the LC₅₀ concentration of emamectin benzoate in systemic bioassays.
200 (A) Ovary development in EB treated BPH at 1, 3, 5 and 7 days after eclosion (DAE) compared
201 to untreated controls. Scale bar = 1,000 μ m. (B) Number of detained eggs in the ovaries of EB
202 treated BPH females measured at 1, 3, 5 and 7 DAE compared to controls. All data are
203 presented as the mean \pm s.e.m. Asterisks indicate values significantly different from the control
204 using student *t* test (ns, no significant; **p* < 0.05 and ***p* < 0.01). (C) Different developmental
205 stages of BPH eggs. (D) No impairment of emamectin benzoate on oogenesis of BPH. Scale
206 bar = 100 μ m.

207

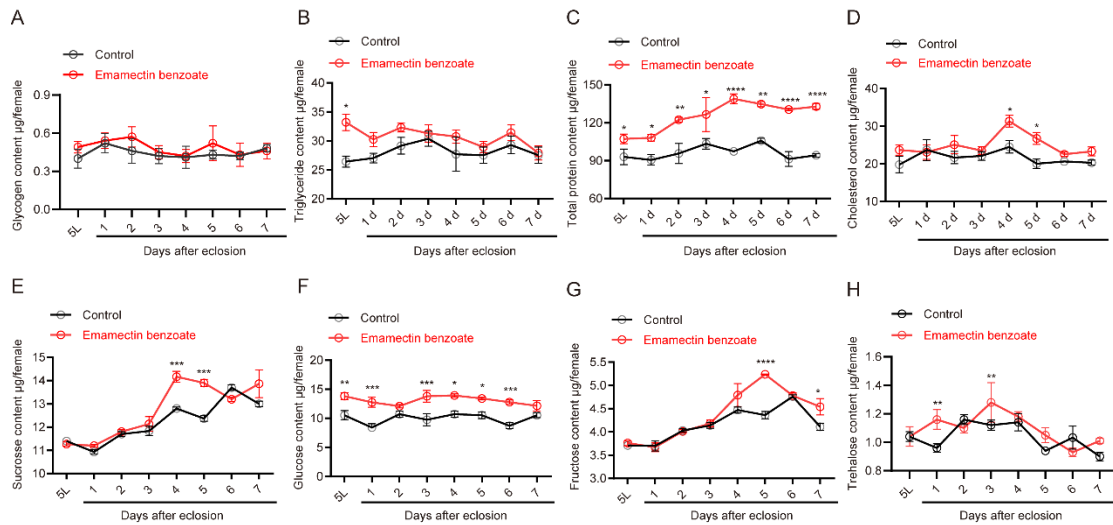
208 **EB exposure enhances the abundances of storage macromolecules and**
209 **circulating sugars in BPH**

210 Nutritional status is an important indicator of reproductive fitness. Thus, to
211 investigate whether EB affects intermediary metabolism and energy storage of BPH,
212 glycogen, triacylglyceride (TAG), total protein content, cholesterol and four circulating
213 carbohydrates were quantified in 4th instar BPH nymphs following exposure to the
214 LC₅₀ of EB.

215 We found that EB exposure has no impact on glycogen levels ([Figure 2-figure](#)
216 [supplement 1A](#)). The amounts of TAG in EB-treated BPH were 27% higher ($p < 0.05$)
217 than those in controls, but only in BPH of the late fifth instar (5L) stage, with no
218 significant differences observed in subsequent developmental stages ([Figure 2-figure](#)
219 [supplement 1B](#)). The amount of total protein content in EB-treated BPH was higher
220 than the control groups in the case of all developmental stages from 5L nymph to
221 7DAE ([Figure 2-figure supplement 1C](#)). EB exposure also increased cholesterol
222 levels at 4 and 5 DAE ([Figure 2-figure supplement 1D](#)). Compared with the solvent
223 control, EB treatment caused significant increases ($p < 0.05$) in the levels of sucrose,
224 glucose, fructose, and trehalose ([Figure 2-figure supplement 1E-H](#)). Thus,
225 collectively, these data provide evidence that EB exposure leads to energy
226 mobilization and the metabolism of carbohydrates and lipids in BPH.

227

228 **Figure 2-figure supplement 1**



229

230 **Figure 2-figure supplement 1.** Amounts of Glycogen (A), TAG (B), total protein content (C),
231 cholesterol (D) and four circulating sugars including sucrose, glucose, fructose and trehalose
232 (E-H) after BPH exposure to EB. All data are presented as the mean \pm s.e.m. The differences
233 between the EB-treated and solvent-treated BPH were analyzed using unpaired student *t*-test
234 (*, $p < 0.05$; **, $p < 0.01$; ***, $p < 0.001$; ****, $p < 0.0001$).

235

236 **EB stimulates egg-laying that is mediated by the JH signaling pathway**

237 Given the important role of juvenile hormone (JH) in vitellogenesis and egg
238 development in insects [19, 25, 27-29], we asked whether EB-treatment could
239 influence the titer of JH in BPH. As measured by ELISA, the juvenile hormone titer of
240 BPH nymphs treated with the LC₅₀ concentration of EB was significantly lower than
241 that of controls in systemic bioassays during the middle and late stages of the 4th
242 instar (Figure 3A). However, at 2, 3 and 4 DAE, the JH titer in the EB treated group
243 was significantly higher than that of the control (Figure 3A). Interestingly, the titer of
244 another important insect hormone, the steroid ecdysone, was not significantly
245 different between EB-treated BPH and solvent-treated controls (Figure 3-figure

246 [supplement 1](#)). To independently validate the results of ELISA assays, we employed
247 HPLC-MS/MS to measure JH titer in BPH following EB exposure [27, 30, 31]. The
248 results showed that JH III titer significantly decreased after EB-treatment at the late
249 4th instar nymph stage (Figure 3A and B), but significantly increased at the third day
250 after eclosion (3 DAE) (Figure 3A and C). To further investigate the role of JH in EB-
251 enhanced fecundity in BPH, we treated BPH with methoprene and pyriproxyfen, JH
252 analogues or biologically active JH mimics respectively, to determine whether they
253 can stimulate fecundity in BPH. Both compounds significantly increased egg-laying in
254 BPH (Figure 3D). Taken together these results reveal that EB stimulates an
255 increased in JH titer that induces fecundity in BPH. Since we found that EB could
256 induce JH synthesis in the BPH, we asked whether EB could influence the
257 expression of genes that are involved in JH synthesis or degradation. For this we
258 treated 4th instar nymphs of BPH with the LC₅₀ concentration of EB using systemic
259 bioassays, and then collected early (5E), middle (5M) and late (5L) stage of 5th instar
260 nymph and 1-7 DAE female adults (DAE) for analysis. Quantitative PCR was then
261 used to examine the expression of key genes previously implicated in the regulation
262 of JH [32, 33].

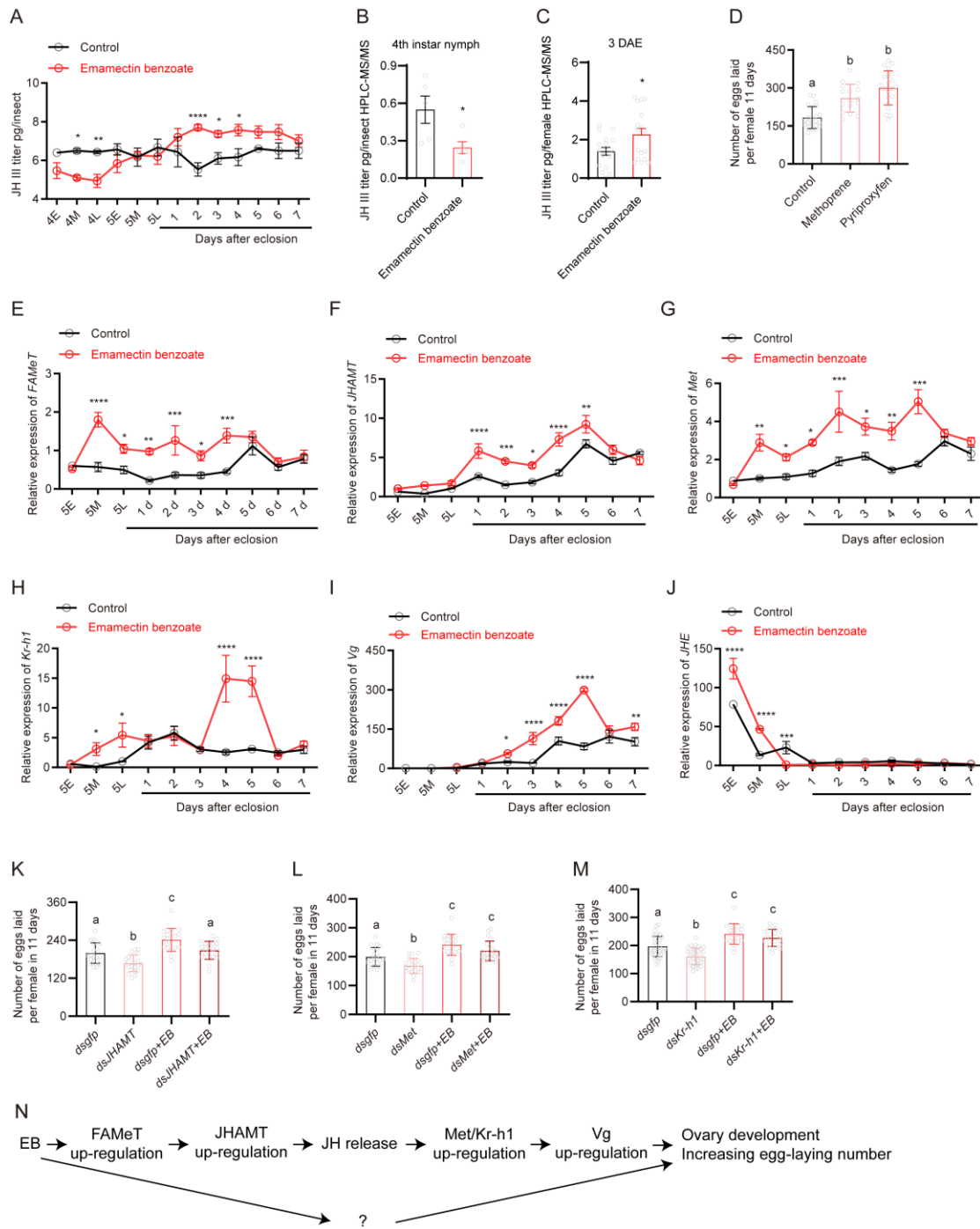
263 Farnesoic acid O-methyltransferase (FAMeT) [34], is known as an important
264 enzyme in the JH biosynthetic pathway, catalyzing methylation of farnesoic acid (FA)
265 to methyl farnesoate (MF) [33]. We found that this gene was significantly upregulated
266 in 5M instar nymph to 4 DAE after EB- treatment (1.0-fold to 3.0-fold) (Figure 3E).
267 Another gene, juvenile hormone acid methyltransferase (JHAMT) [33, 35], which is

268 involved in the biosynthesis of JH, was also upregulated in EB-treated BPH at 1 to 5
269 DAE than controls (1.5-fold to 3.0-fold) (Figure 3F). Methoprene-tolerant (*Met*),
270 belongs the basic helix–loop–helix Per/Arnt/Sim (bHLH-PAS) family of transcription
271 factors and is the intracellular (nuclear) receptor of JH [36, 37]. The levels of *met*
272 mRNA increased in EB-treated BPH at the 5M and 5L instar nymph and 1 to 5 DAE
273 stages compared to controls (1.7-fold to 2.9-fold) (Figure 3G). Krüppel homolog 1
274 (*Kr-h1*), a transcriptional target of JH signaling, is reported to be sensitive to levels of
275 JH and its expression levels are directly correlated with JH titers [32, 38, 39]. We
276 found that *Kr-h1* was significantly upregulated in the adults of EB-treated BPH at the
277 5M, 5L nymph and 4 to 5 DAE stages (4.7-fold to 27.2-fold) (Figure 3H). Similarly, the
278 expression levels of vitellogenin (*Vg*), a key downstream component of JH signaling
279 triggering ovary development in insects including BPH [40], was markedly increased
280 in females at 2–5 DAE by EB (1.7-fold to 5.5-fold) (Figure 3I). Juvenile hormone
281 esterase (*JHE*) is the primary JH-specific degradation enzyme that plays a key role in
282 regulating JH titers [41]. Interestingly, we observed a significant upregulation of *JHE*
283 mRNA levels in the early and middle 5th instar nymph stage followed by
284 downregulation in 5L instar nymphs of EB-treated BPH (1.3-fold to 2.6-fold) (Figure
285 3J). In combination these results reveal that EB has profound impacts on the
286 expression of key genes involved in the synthesis of JH or downstream signaling
287 pathway genes that might promote egg development.

288 To further understand whether these JH pathway-related genes were involved in
289 egg-laying behavior in BPH, we performed RNAi experiments to downregulate the

290 expression of *JHAMT*, *Met* and *Kr-h1* (Figure 3-figure supplement 2A-C). We found
291 that silencing of these three genes downregulated the titer of JH in BPH providing
292 functional evidence of their role in the regulation of JH (Figure 3-figure supplement
293 2D). Furthermore, silencing of *Kr-h1* inhibited *FAMeT* and *Vg* gene expression while
294 increasing *JHE* gene expression (Figure 3-figure supplement 2E-H). Importantly,
295 silencing of *JHAMT*, *Met* and *Kr-h1* gene in female BPH was also found to suppress
296 egg-laying (Figure 3K-M). However, this phenotype was rescued by EB treatment,
297 which restored egg-laying to normal levels in BPH injected with *JHAMT*, *Met* and *Kr-*
298 *h1* dsRNA (Figure 3K-M). Together these results provide a mechanistic
299 understanding of how EB enhances fecundity in BPH by modulating the expression
300 of key genes involved in JH synthesis (Figure 3N).
301

302 **Figure 3**



303

304 **Figure 3. EB induced reproduction in BPH is mediated by components of the JH**

305 **signaling pathway.** (A) The titer of JH III (as measured by ELISA assay) at different

306 developmental stages of BPH when 4th instar nymphs were treated with the median lethal

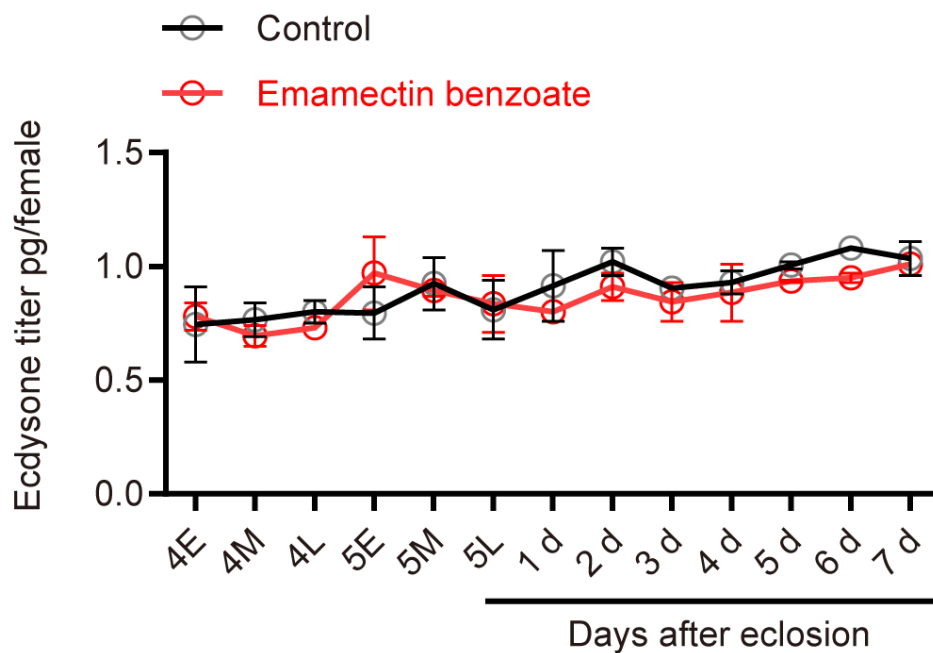
307 concentrations of EB. (B and C) The titer of JH III (as measured by HPLC-MS/MS) in BPH

308 females at 4L and 3 DAE when treated with median lethal concentrations of EB. (D) Oviposition

309 rate of BPH when 4th instar nymphs were treated with 4 ppm methoprene or 10 ppm

310 pyriproxyfen. (E-J) Expression of selected JH-related genes (*FAMeT*, *JHAMT*, *Met*, *Kr-h1*, *Vg*,
311 and *JHE*) in EB-treated BPH. (K) Egg production following silencing of *JHAMT* with or without
312 EB application. (L) Egg production following silencing of *met* with or without EB application. (M)
313 Egg production after silencing *Kr-h1* with or without EB application. (N) Schematic illustrating
314 the proposed impact of EB on the JH signaling pathway leading to enhanced reproduction. The
315 question mark indicates one or more potential additional signals. All data are presented as
316 means \pm s.e.m. Student's *t* test was used to compare the two samples. One-way ANOVA with
317 Tukey's multiple comparisons test was used to compare more than two samples. ns, no
318 significant difference; Asterisks indicate values significantly different from the control (ns, no
319 significant; * $p < 0.05$, ** $p < 0.01$, *** $p < 0.001$ and **** $p < 0.0001$). Different lower-case letters
320 above the bars indicate significant differences ($p < 0.05$).

321 **Figure 3-figure supplement 1**



322

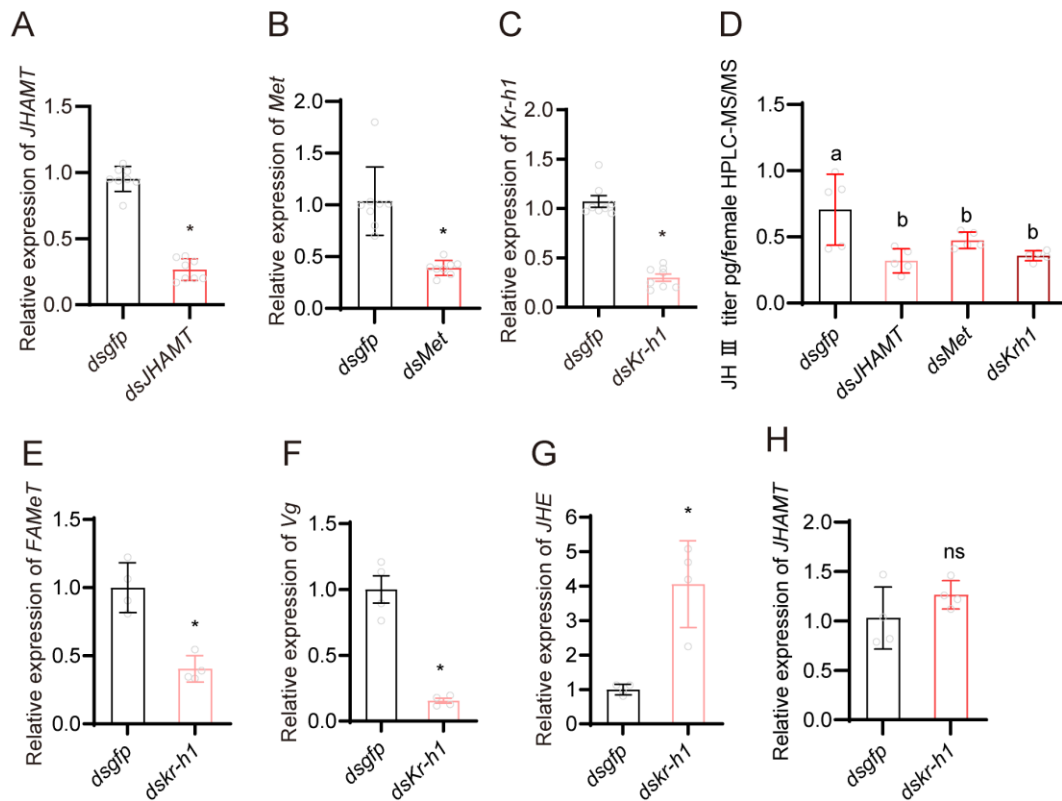
323 **Figure 3-figure supplement 1.** Ecdysone titer at different developmental stages of BPH when

324 4th instar nymphs were treated with median lethal concentrations of EB.

325

326

327 **Figure 3-figure supplement 2**



328

329 **Figure 3-figure supplement 2.** (A-C) Expression of *JHAMT* (A), *Met* (B) and *Kr-h1* (C)

330 following RNAi knockdown. (D) The titer of JHIII (as measured by HPLC-MS/MS) at 3 DAE

331 when female adults were injected with *dsJHAMT*, *dsMet*, and *dsKr-h1* at 1 DAE. (E-H)

332 Expression of *FAMeT*, *Vg*, *JHE* and *JHAMT* when *Kr-h1* was silenced in BPH. All data are

333 presented as means \pm s.e.m. * $p < 0.05$; Mann-Whitney test.

334

335 **EB induces JH biosynthesis through the peptidergic AstA/AstAR signaling**
336 **pathway**

337 The timing and level of JH biosynthesis can be precisely regulated by the
338 neuropeptides, stimulatory allatotropins (ATs) and inhibitory allatostatins (Asts), in
339 many insects [42-49]. Insects can, in a species-specific manner, produce one type of
340 AT and three types of Asts: FGL-amide Ast (AstA) [43, 50]; myoinhibitory peptide
341 (MIP or AstB) and PISCF Ast (AstC) [47, 51]. In some species, there also exists two
342 paralogue genes of AstCs which are named AstCC and AstCCC [52, 53].
343 Interestingly, the allatostatic activity of these three types of Ast peptides varies
344 between insect species so that in each species only one type of Ast (for example
345 AstA) controls JH production [47, 48, 51, 54].

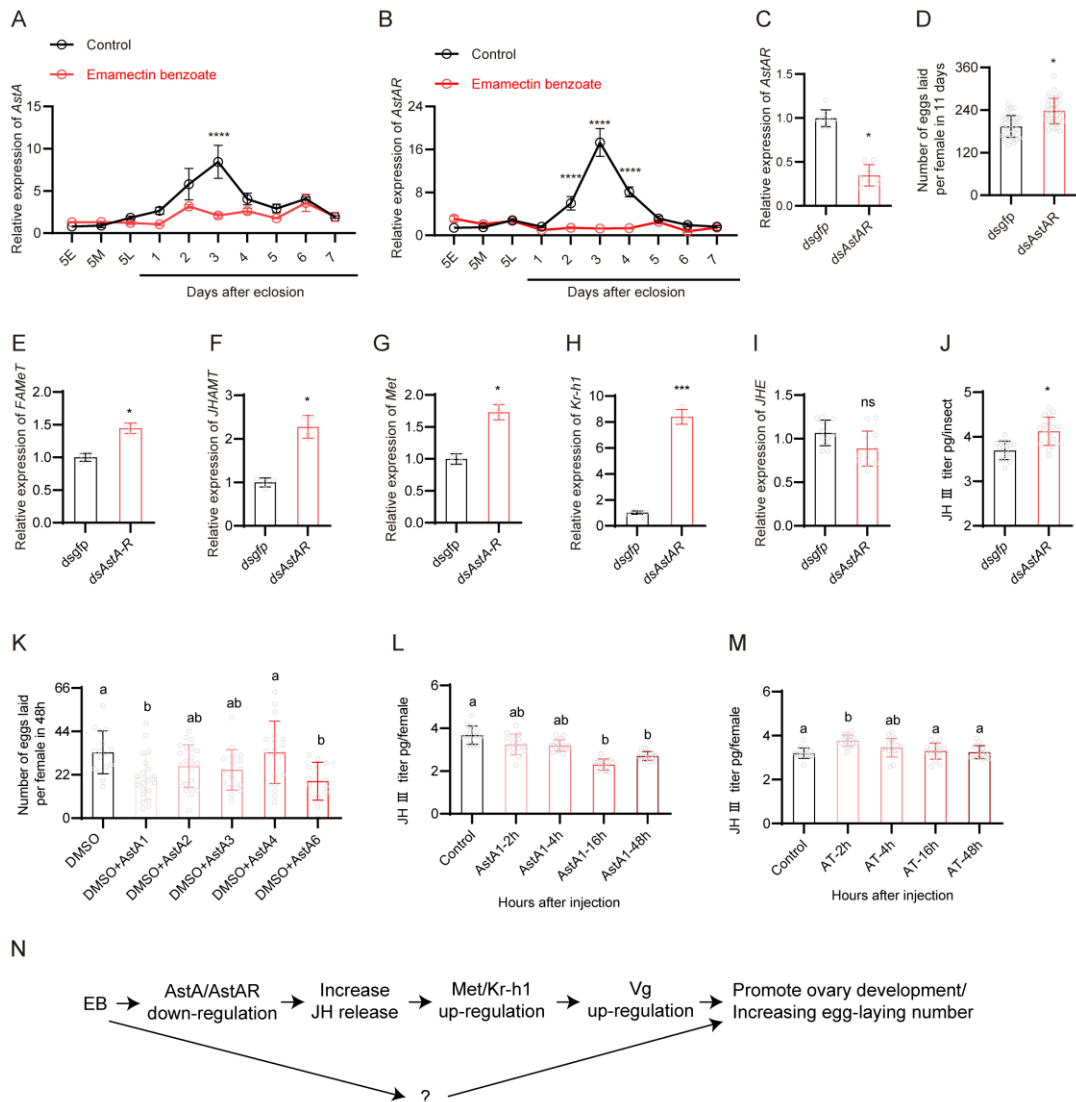
346 Analysis of the BPH neural transcriptome sequence data has revealed the
347 presence of one AT, four types of Asts and four corresponding receptors, allatotropin
348 receptor (A16, ATR), AstA receptor (A2, AstAR), AstB (MIP) receptor (A10, AstBR or
349 MIPR) and AstC receptor (A1, AstCR) [55]. We cloned the five neuropeptide genes
350 (AT, AstA, AstB/MIP, AstCC and AstCCC) and confirmed the sequence obtained from
351 transcriptome data (Figure 4-figure supplement 1) [55]. Interestingly, we found that
352 AstC is missing in the genome of BPH and only AstCC and AstCCC are present
353 (Figure 4-figure supplement 1). Next, we also cloned their corresponding receptors
354 [52] including ATR (A16), AstAR (A2), AstBR (A10) and AstCR (A1) which might be
355 activated by AstCC and/or AstCCC [39, 52, 56]. Sequence alignments and
356 phylogenetic analysis are shown in Figure 4-figure supplement 2.

357 Quantitative PCR was then used to examine if EB treatment could influence the
358 expression of the genes encoding these neuropeptides and their receptors. Treating
359 BPH with the LC₅₀ concentration of EB significantly increased the expression of *AT*,
360 *ATR* and *AstCCC* while resulting in the downregulation of *AstA*, *AstB/mip*, *AstCC*,
361 *AstAR* and *AstBR/mipr* at the adult stage (Figure 4A and B, Figure 4-figure
362 supplement 3A-G). Among these, *AstA* and *AstAR* were the most downregulated
363 genes after EB treatment (Figure 4A and B, Figure 4-figure supplement 3H) and thus
364 the *AstA/AstAR* signaling system was selected for subsequent functional analysis.
365 Silencing of *AstAR* in female BPH using RNAi (Figure 4C), resulted in an increased
366 number of eggs laid per female compared with *dsgfp*-injected controls (Figure 4D).
367 Interestingly, silencing *AstAR* also resulted in the upregulation of *FAMeT*, *JHAMT*,
368 *Met* and *Kr-h1* which are involved in the JH biosynthesis/signaling (Figure 4E-H).
369 However, *JHE* was not influenced by *AstAR* silencing (Figure 4I). We therefore
370 investigated whether silencing the *AstAR* gene could influence JH titer in BPH. A
371 significantly increased JH titer was observed in *AstAR* silenced BPH compared with
372 controls (Figure 4J). Thus, our data strongly suggest that *AstA* is a key inhibitor of JH
373 production in BPH.

374 Finally, we investigated whether injection of mature *Ast* and *AT* peptides could
375 influence the number of eggs laid and JH titer in BPH. We synthesized one *AT*, six
376 *AstAs* (*AstA1* to *AstA6*), one *AstCC* and one *AstCCC* peptide according to their
377 determined sequences (Figure 4-figure supplement 1). Indeed, we found that
378 injection of *AstA1* and *AstA6* reduced the number of eggs laid per female in 48 h

379 (Figure 4K). We also observed that AstA1 injection after 16h and 48h decreased the
380 JH titer significantly (Figure 4L), and AT injection increased the JH titer after 2h but
381 levels returned to normal after 4h injection (Figure 4M). Collectively, these results
382 provide compelling evidence that EB induces reproduction in BPH through the
383 AstA/AstAR and JH signaling pathways (Figure 4N) and further supports the role of
384 AstA and AT in regulation of JH titer.

385 **Figure 4**



386

387 **Figure 4. EB induced reproduction in BPH is mediated by the AstA/AstAR and JH**
 388 **signaling pathway.**

389 (A and B) Expression of *AstA* and *AstAR* in different stages of BPH following EB treatment. (C)

390 Downregulation of *AstAR* using RNAi leads to a reduction in mRNA expression level. (D) Egg

391 production in female BPH following silencing of *AstAR* gene. (E-I) Expression of selected JH

392 signaling pathway related genes (*FAMeT*, *JHAMT*, *Met*, *Kr-h1* and *JHE*) in *AstAR* silenced BPH.

393 (J) JHIII titer of BPH females after *AstAR* gene silencing determined by HPLC-MS/MS. (K)

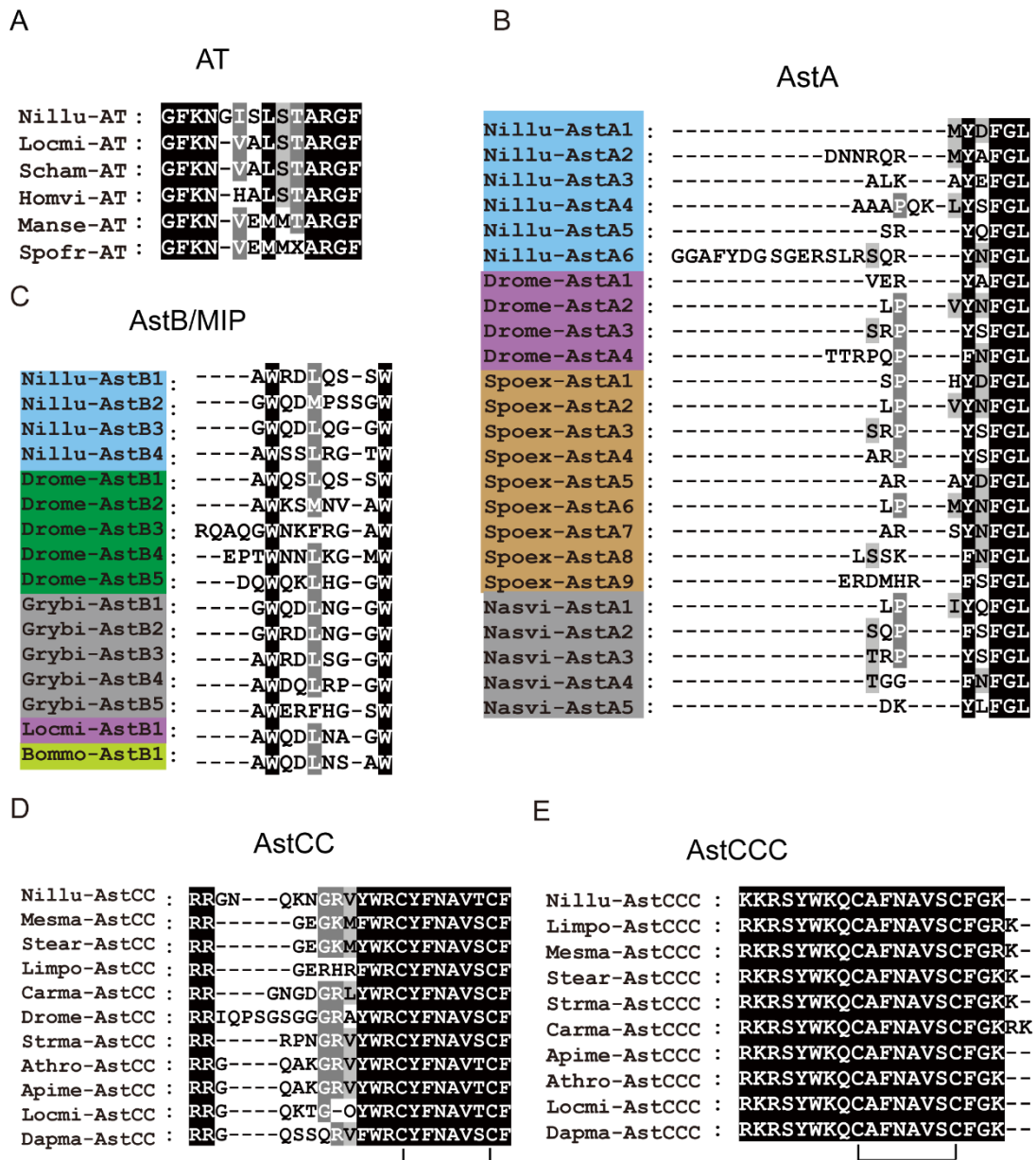
394 Number of eggs laid per female in 48h following injection of six AstA1-AstA6 mature peptides

395 and one AT mature peptide. Fifty nanoliter of PBS (as control) and seven peptides (20

396 pmol/insect) were injected into female BPH three days after eclosion. (L and M) The JH III titer

397 of BPH females at different time points following AstA or AT injection. (N) Schematic of the
398 proposed role of AstA/AstAR in the regulation of JH following EB exposure. The question
399 mark indicates one or more possible additional signals. All data are presented as means \pm s.e.m.
400 Student's *t* test was used to compare the two samples. One-way ANOVA with Tukey's multiple
401 comparisons test was used to compare more than two samples. ns, no significant difference;
402 Asterisks indicate values significantly different from the control (ns, no significant; * $p < 0.05$, ** p
403 < 0.01 , *** $p < 0.001$ and **** $p < 0.0001$). Different lower-case letters above the bars indicate
404 significant differences ($p < 0.05$).
405

406 **Figure 4-figure supplement 1**

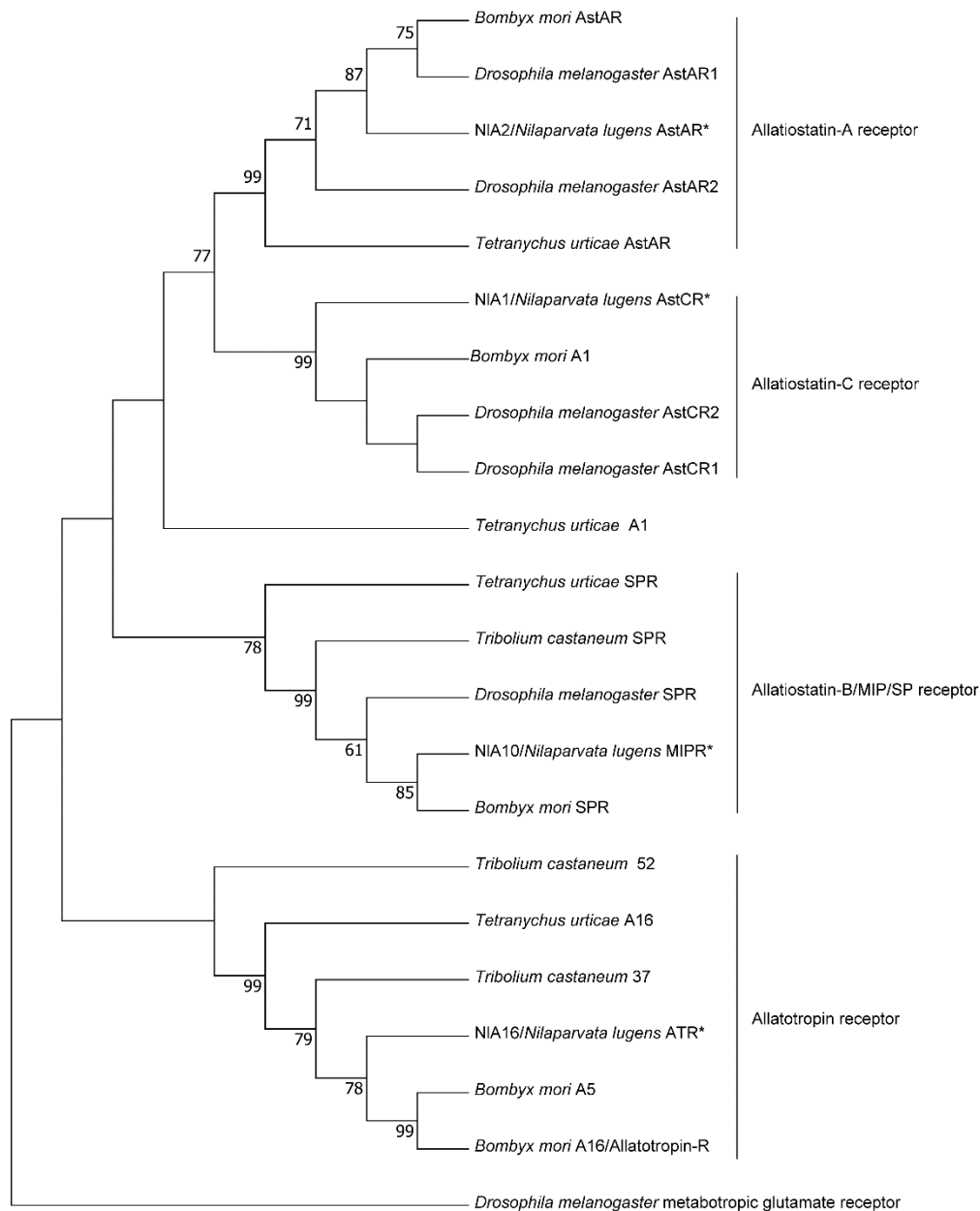


407

408 **Figure 4-figure supplement 1.** Alignments of the amino acid sequences of: (A) AT, (B) AstA,
 409 (C) AstB/MIP, (D) AstCC and (E) AstCCC peptides from select species. AT, AstA, AstB/MIP and
 410 AstCCC are predicted to have a C-terminal amide. The mature peptides belonging to the same
 411 species have been highlighted with the same color. Species names are as follows: Nillu
 412 (*Nilaparvata lugens*), Locmi (*Locusta migratoria*), Scham (*Schistocerca americana*), Homvi
 413 (*Homalodisca vitripennis*), Manse (*Manduca sexta*), Spofr (*Spodoptera frugiperda*), Drome
 414 (*Drosophila melanogaster*), Spoex (*Spodoptera exigua*), Nasvi (*Nasonia vitripennis*), Grybi
 415 (*Gryllus bimaculatus*), Bommi (*Bombyx mori*); Mesma (*Mesobuthus martensii*), Stear

416 (*Stegodyphus araneomorph*), Limpo (*Limulus polyphemus*), Carma (*Carcinus maenas*), Strma
417 (*Strigamia maritima*), Athro (*Athalia rosae*), Apime (*Apis mellifera*), Dapma (*Daphnia magna*).
418 Black lines under the sequences indicate the locations of the disulfide bridges in the mature
419 peptides. The accession numbers of the sequences are listed in Figure 4-figure supplement 1
420 source data.
421

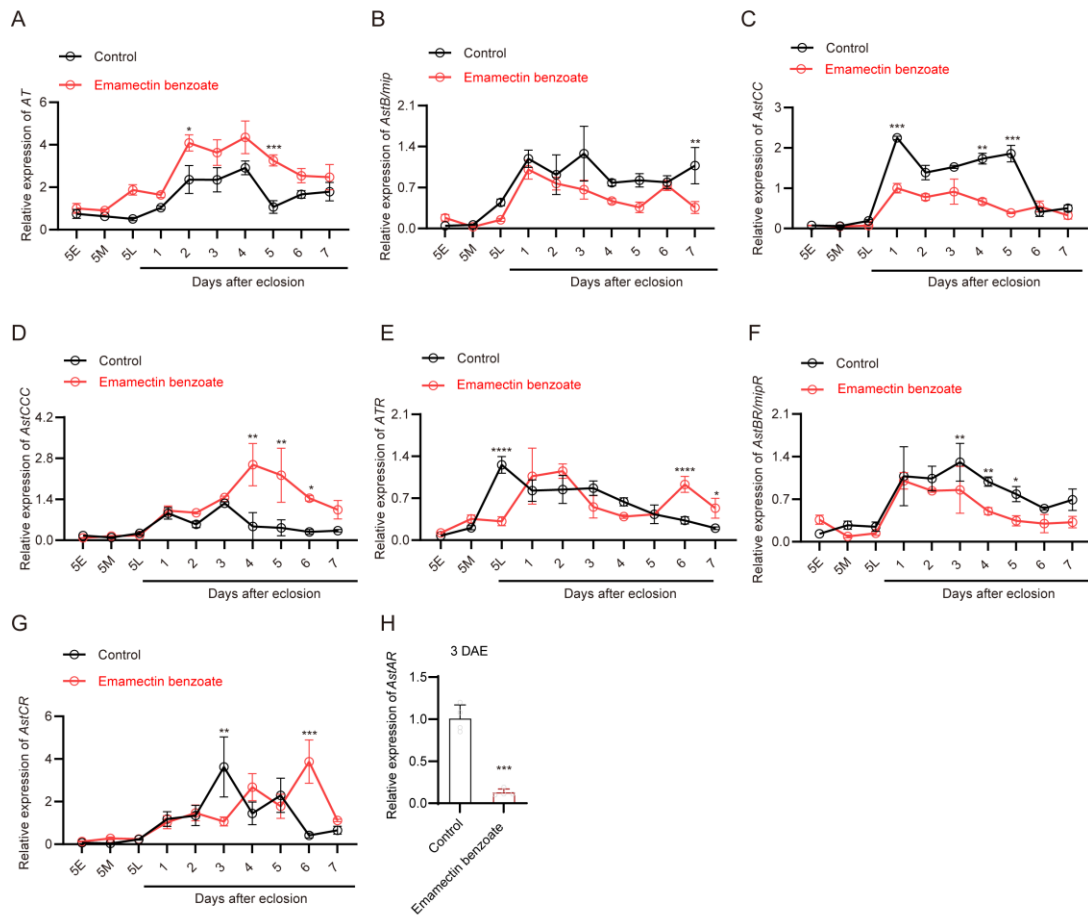
422 **Figure 4-figure supplement 2**



423

424 **Figure 4-figure supplement 2.** Phylogenetic tree of the predicted BPH (*) allatotropin receptor
425 (A16, ATR), allatostatins A receptor (A2, AstAR), AstB (MIP) receptor (A10, AstBR or MIPR)
426 and allatostatins C receptor (A1, AstCR) with other insect species. The tree was generated
427 using the maximum likelihood method. *Drosophila melanogaster* metabotropic glutamate
428 receptor was included as an outgroup. The accession numbers of the sequences used for this
429 phylogenetic tree are listed in Figure 4-figure supplement 2 source data.

430 **Figure 4-figure supplement 3**



431

432 **Figure 4-figure supplement 3. EB induced changes in the expression of AT, AstB, AstCC,**

433 **AstCCC, ATR, AstBR and AstCR in BPH.** All data are presented as means \pm s.e.m. Student's

434 t test was used to compare the two samples. ns, no significant difference; Asterisks indicate

435 values significantly different from the control (* p < 0.05, ** p < 0.01, and *** p < 0.001).

436

437 **EB-enhanced fecundity in BPH is dependent on its molecular target protein the**

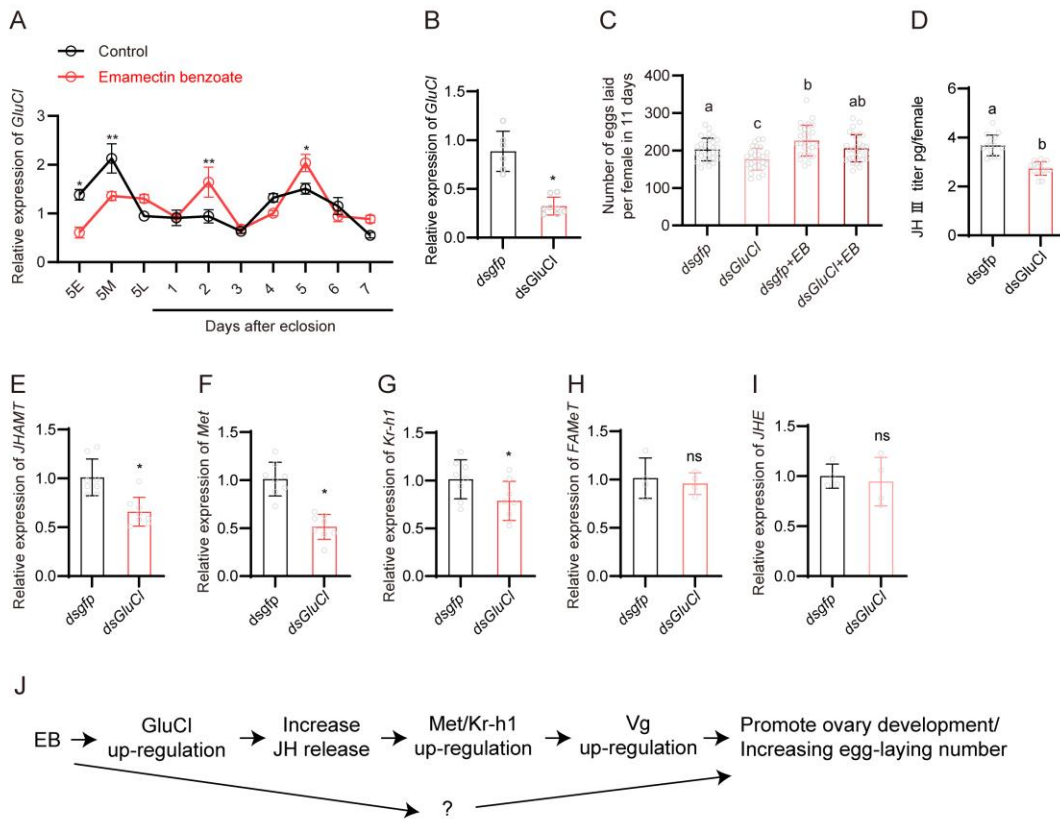
438 **GluCl**

439 EB and abamectin, are allosteric modulators, which target glutamate-gated
440 chloride channels (GluCls) [57-59]. Hence, we examined whether EB-stimulated
441 fecundity in BPH is influenced by its molecular target GluCl. The full length *GluCl*
442 coding sequence from BPH was cloned and sequenced (Figure 5-figure supplement
443 1) and the impact of EB on *GluCl* gene expression examined using quantitative PCR.
444 Treatment of BPH with the LC₅₀ concentration of EB significantly downregulated
445 *GluCl* gene expression at the 5E and 5M nymph stages while upregulating *GluCl*
446 gene expression at 2 DAE and 5 DAE in the adult stage (Figure 5A). To examine the
447 role of *GluCl* gene in BPH fecundity, RNAi was used to knockdown expression of this
448 gene in female BPH (Figure 5B). A significant decrease in the number of eggs laid by
449 per female was observed in *dsGluCl*-injected insects compared with *dsgfp*-injected
450 insects (Figure 5C). However, treatment with EB was found to rescue the decreased
451 egg-laying phenotype induced by *dsGluCl* injection (Figure 5C). To investigate the
452 mechanism by which *GluCl* expression modulates fecundity we examined if silencing
453 *GluCl* influences JH titer and JH-related gene expression. Indeed, we observed that
454 RNAi knockdown of *GluCl* leads to a decrease in JH titer (Figure 5D) and down-
455 regulation of genes including *JHAMT* which is responsible for JH synthesis, and the
456 JH signaling downstream genes *Met* and *Kr-h1* (Figure 5E-G). In contrast,
457 expression of *FAMeT* and *JHE* were not changed in the *GluCl* silencing insects
458 (Figure 5H and I). We also examined whether silencing *GluCl* impacts the

459 *AstA/AstAR* signaling pathway. Silencing *GluCI* was found to have no impact on the
460 expression of *AT*, *AstA*, *AstB*, *AstCC*, *AstAR*, and *AstBR*. However, the expression of
461 *AstCCC* and *AstCR* was significantly upregulated in *dsGluCI*-injected insects ([Figure](#)
462 [5-figure supplement 2A-H](#)). These results suggest that EB activates *GluCI* which
463 induces JH biosynthesis and release, which in turn stimulates reproduction in BPH
464 ([Figure 5J](#)).

465

466 **Figure 5**

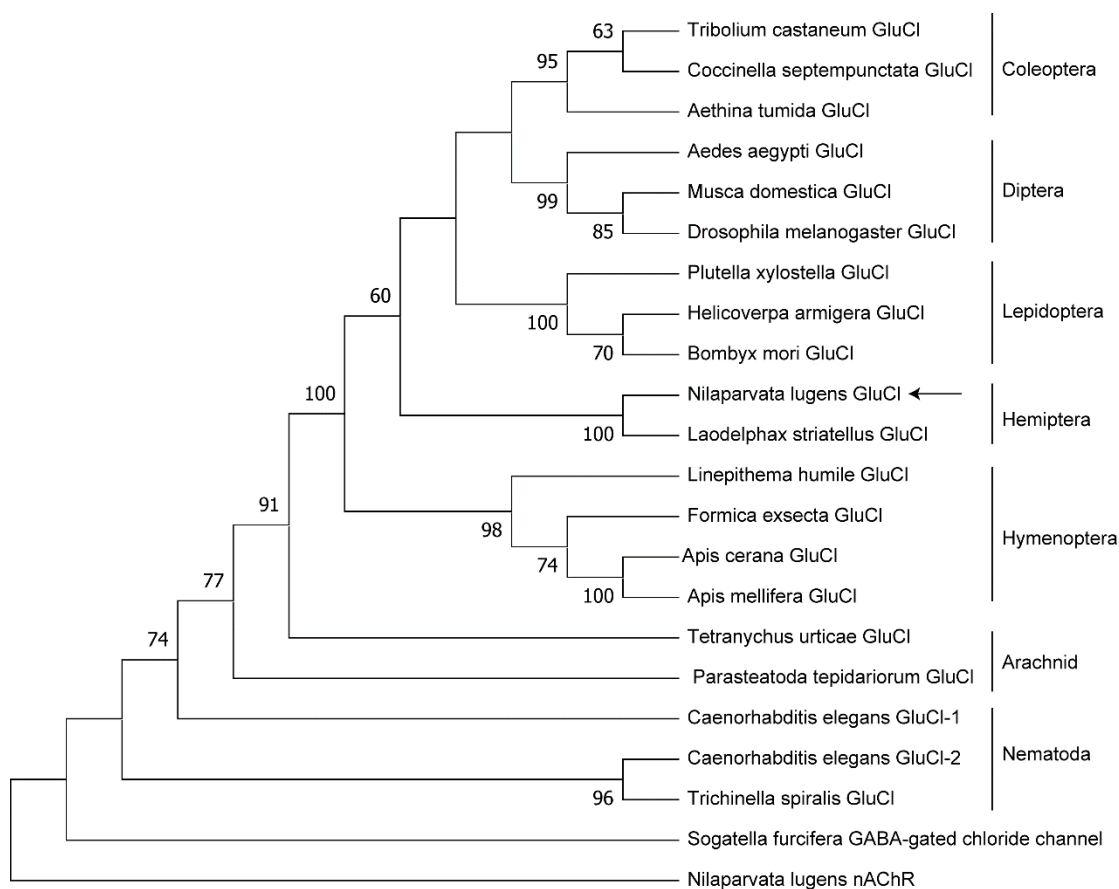


467

468 **Figure 5. EB induced reproduction in brown planthoppers through its molecular target**
 469 **protein GluCI.**

470 (A) Expression of *GluCI* in EB-treated and untreated BPH. (B) Expression of *GluCI* following
 471 injection of *dsGluCI* in BPH. (C) Egg production after *GluCI* gene knockdown in EB-treated and
 472 untreated BPH. (D) The JH III titer of BPH females after *GluCI* gene silencing as quantified
 473 using the ELISA method. (E-I) Expression patterns of selected JH-related genes (*JHAMT*,
 474 *Met*, *Kr-h1*, *FAMEt* and *JHE*) in *GluCI* silenced BPH. (J) Schematic of the proposed role of *GluCI* as
 475 a molecular target of EB and EB-enhanced reproduction in BPH. The question mark indicates
 476 one or more possible additional signals. All data are presented as means \pm s.e.m. Student's t
 477 test was used to compare the two samples. One-way ANOVA with Tukey's multiple
 478 comparisons test was used to compare more than two samples. ns, no significant difference;
 479 Asterisks indicate values significantly different from the control (ns, no significant; * $p < 0.05$ and
 480 ** $p < 0.01$). Different lower-case letters above the bars indicate significant differences ($p < 0.05$).

481 **Figure 5-figure supplement 1**

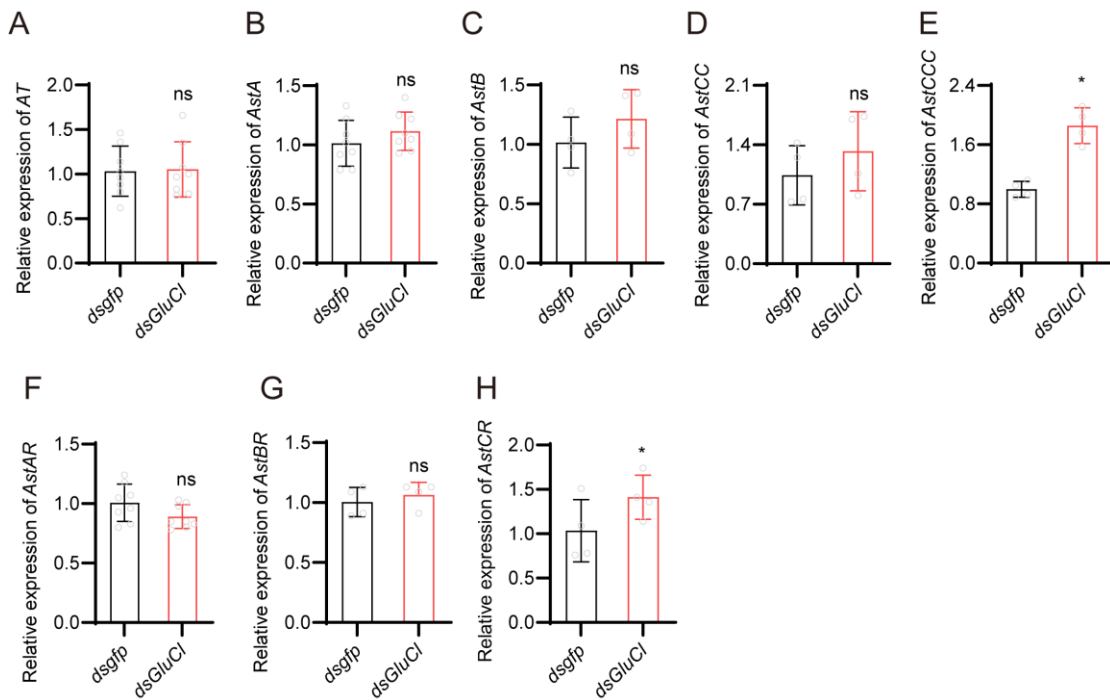


482

483 **Figure 5-figure supplement 1.** Phylogenetic analysis of glutamate-gated chloride channels in
484 different species. The numbers at the nodes of the branches represent the percentage
485 bootstrap support (1000 replications) for each branch. The *Sogatella furcifera* GABA-gated
486 chloride channel and *Nilaparvata lugens* nAChR were used as outgroup. Alignment was
487 performed with amino acid sequences from TM1-7. The receptor names are listed in the tree.
488 The accession numbers of the sequences used for this phylogenetic tree are listed in [Figure 5-](#)
489 [figure supplement 1 source data](#).

490

491 **Figure 5-figure supplement 2**



492

493 **Figure 5-figure supplement 2.** The expression of *AT*, *AstA*, *AstB*, *AstCC*, *AstCCC*, *AstAR*,

494 *AstBR* and *AstCR* in BPH injected with *dsGluCI* or *dsGfp*. All data are presented as means \pm

495 s.e.m. Student's *t* test was used to compare the two samples. ns, no significant. Different lower-

496 case letters above the bars indicate significant differences ($p < 0.05$).

497

498 **Discussion**

499 Pesticide-induced resurgence of pest insects is a serious problem in rice and
500 several other cropping systems [3]. However, the mechanisms underpinning pesticide-
501 enhanced reproduction in insects remain poorly understood. Here we reveal that a
502 suite of molecular actors underlie this trait that, in combination, mediate profound
503 physiological changes in the reproductive fitness of female BPH. Our data provide
504 fundamental insights into the molecular mechanisms by which xenobiotics modify
505 insect reproduction and have applied implications for the control of a highly damaging
506 crop pest. We discuss these topics below.

507

508 **Sublethal doses of GluCl modulators, EB and abamectin, stimulates fecundity in** 509 **BPH**

510 We show that in both contact and systemic assays EB and abamectin stimulate
511 reproduction in BPH. Thus, insecticide-enhanced reproduction is likely a key factor in
512 the BPH resurgence observed when farmers use EB and abamectin to control
513 leaffolders in rice crops in China [26]. Although this is the first report of sublethal doses
514 of avermectins enhancing insect fecundity, our findings are consistent with previous
515 studies which have shown that certain insecticides, herbicides and fungicides stimulate
516 BPH reproduction [3, 7, 14, 60-65]. Intriguingly, we show that EB only induces fecundity
517 in female adults and is specific to BPH, with EB exposure failing to enhance
518 reproduction in two related species, the small brown planthopper, *L. striatellus* and the
519 white backed planthopper, *S. furcifera*, or the model insect *D. melanogaster*. Thus, the

520 mechanisms underpinning this trait appear to act exclusively on female BPH and may
521 be specific to this species.

522 Pesticides may stimulate insect reproduction through a variety of physiological and
523 molecular mechanisms. Our data reveal that exposure to sub-lethal concentrations of
524 EB results in profound changes to female BPH fitness, leading to increases in female
525 weight, total protein content, cholesterol content, sugar content and egg production
526 and decreases in duration of the preoviposition period. Some of these findings exhibit
527 parallels with previous studies, which demonstrated that treating third-instar BPH
528 nymphs with either deltamethrin, triazophos, or imidacloprid led to increased soluble
529 sugar levels in the corresponding adults [66]. Such metabolites provide the energy that
530 drives BPH reproduction and resurgence [3]. Thus, together with prior work, our results
531 suggest that pesticides associated with resurgence stimulate nutritional intake in BPH
532 to fuel enhanced energy-intensive reproduction.

533

534 **The JH signaling pathway plays an essential role in EB-induced fecundity in BPH**

535 JH is a pleiotropic hormone which plays important roles in development and
536 reproduction in insects [19, 67]. Circulating JH titers are regulated by factors that
537 control JH production in the corpora allata including biosynthetic enzymes and
538 catabolic enzymes that regulate JH levels. Our results show that EB increases
539 circulating JH III titers in BPH females over 2–4 days after eclosion (DAE) and
540 promotes ovary development. Previous studies have reported that triazophos and
541 deltamethrin treatments also lead to increased circulating JH III titers in BPH females

542 over 1–3 days post emergence. Similarly, jinggangmycin treatments were found to lead
543 to increased JH titers (by approximately 45–50%) in BPH females over two days post
544 emergence [68]. Thus our findings, in combination with these previous studies,
545 demonstrate that insecticide treatments can have dramatic effects on the regulation of
546 key insect hormones involved in pest reproduction which can in turn drive pesticide
547 resurgence.

548 Although increased JH titers following pesticide exposure have been correlated
549 with reduced levels of active JH esterase during the first three days PE [6], the type
550 and number of mechanisms mediating the observed increase in hormone titer has
551 remained an open question. Our data reveal that elevated JH titer in EB-exposed BPH
552 is associated with the upregulation of genes that encode biosynthetic enzymes for JH
553 (*JHAMT*) and downstream signaling genes that can induce *vg* gene expression (*met*
554 and *kr-h1*). Using RNAi we provide functional evidence of the role of these genes in
555 the regulation of JH III and fecundity of female BPH, and demonstrate that EB can
556 restore the reduction in egg production resulting from the knockdown of *JHAMT*, *met*
557 and *kr-h1* expression.

558 JHAMAT is an enzyme that catalyzes the conversion of inactive precursors of JH to
559 active JH in the final stages of JH biosynthesis [33, 35]. Interestingly, while it has not
560 been previously implicated in pesticide resurgence, treatment of the stored product
561 pest *Sitotroga cerealella* with diallyl trisulfide, an insecticidal compound in garlic
562 essential oil, was found to increase JHAMT mRNA levels [69]. Because JHAMAT is the
563 key rate-limiting enzyme in regulation of JH titer our results suggest that its enhanced

564 expression is a key molecular mechanism of pesticide resurgence in BPH.

565 Met is a ligand-activated member of the basic helix–loop–helix Per/Arnt/Sim
566 (bHLH-PAS) transcription factors and is the intracellular receptor for JH [36, 37]. Kr-h1
567 is a zinc finger protein that acts downstream of Met and is expressed in response to
568 JH signaling. Although the genes encoding these proteins have not been previously
569 linked to pesticide resurgence, our finding that they are upregulated following EB
570 exposure, and demonstration of their role of in promoting fecundity, is consistent with
571 previous studies. Specifically, treatment of BPH with JH III or the insecticidal analogues
572 methoprene or pyriproxifen was found to induce the expression of *Kr-h1* [70].
573 Furthermore, knockdown of *Met* and *Kr-h1* in BPH brachypterous females was found
574 to result in delayed ovariole development and this was significantly more pronounced
575 than the response observed in BPH treated separately with ds*NIMet* or ds*NIKr-h1* [71].
576 This finding provides evidence of a possible interaction between *Met* and *Kr-h1* and,
577 in combination with our data, suggests that *Met* and *Kr-h1* may act in concert to
578 mediate EB-enhanced fecundity.

579

580 **EB-induced fecundity in BPH is dependent on the allatostatin signaling pathway**

581 In addition to regulatory proteins that promote JH production, insects have
582 peptides that inhibit JH biosynthesis. These include the allatostatins: FGLamides
583 (FGLa; AstA), the W(X)6Wamides (AstB), and the PISCFs (AstC) [47, 48, 54, 55, 72,
584 73]. Interestingly, our results showed that EB exposure results in the marked
585 downregulation of the expression of the genes encoding allatostatin *AstA* and its

586 receptor *AstAR*. We provide clear evidence of the functional impact of this on JH
587 synthesis and BPH fecundity by: i) demonstrating that RNAi knockdown of *AstAR*
588 expression results in increased JH titer and enhanced female egg production, and, ii)
589 showing that injection of female BPH with synthetic ASTa peptide reduces JH titer and
590 decreases egg production. Thus, our data provide unequivocal evidence that AstA is a
591 key inhibitor of JH production in BPH. This finding is consistent with previous work
592 which has shown that FGLa/ASTs inhibit JH biosynthesis in cockroaches, and termites
593 [43, 74]. To our knowledge, our study is the first report of insecticides inhibiting the
594 expression of the neuropeptide receptor, *AstAR*, and linking this to increases in JH titer
595 and enhanced reproduction in insects.

596 Interestingly knockdown of *AstAR* resulted in significant increases in the
597 expression of genes involved in JH synthesis/signaling including *FAMeT* and *JHAMT*
598 *Met* and *Kr-h1*. Related to this finding, previous work has shown that knockdown of the
599 AstA receptor gene, *Dar-2*, in *D. melanogaster* results in changes in the expression of
600 genes encoding Drosophila insulin-like peptides (DILPs) and adipokinetic hormone
601 (AKH) signaling proteins [75]. Together with our findings, this demonstrates that AstA
602 receptors may modulate the expression of numerous downstream genes involved in
603 metabolism, energy store and reproduction. In the case of pesticide resurgence our
604 results imply significant cross-talk in the expression of genes that inhibit JH production
605 and those that promote it.

606

607 **The GluCl plays an essential role in EB-induced fecundity in BPH**

608 EB and abamectin are allosteric modulators of GluCl_s [57-59]. Our data revealed
609 that EB exposure modifies expression of the GluCl in BPH, and knockdown of GluCl
610 expression resulted in a reduction in both JH levels and egg production. Interestingly,
611 the GluCl has been reported to inhibit the biosynthesis of JH in the cockroach,
612 *Diploptera punctata* [76]. Recent work has also reported that modulation of
613 glutamatergic signals may contribute to the photoperiodic control of reproduction in
614 bean bug, *Riptortus pedestris* [77]. Interestingly, work on *D. punctata* has revealed that
615 application of the GluCl channel agonist ivermectin, which like EB belongs to the
616 avermectin family, caused a decline in JH synthesis in corpus allatum glands [76].
617 While the inhibitory effect of ivermectin observed in this previous study differs from the
618 activating effect of EB we observed in our study, it is consistent with our finding of a
619 role for GluCl channel in the regulation of JH regulation. Interestingly, we found that
620 knockdown of *GluCl* gene expression results in the down-regulation of *JHAMT*, *Met*
621 *and Kr-h1*, further revealing significant convergent relationships between genes
622 underpinning pesticide resurgence.

623

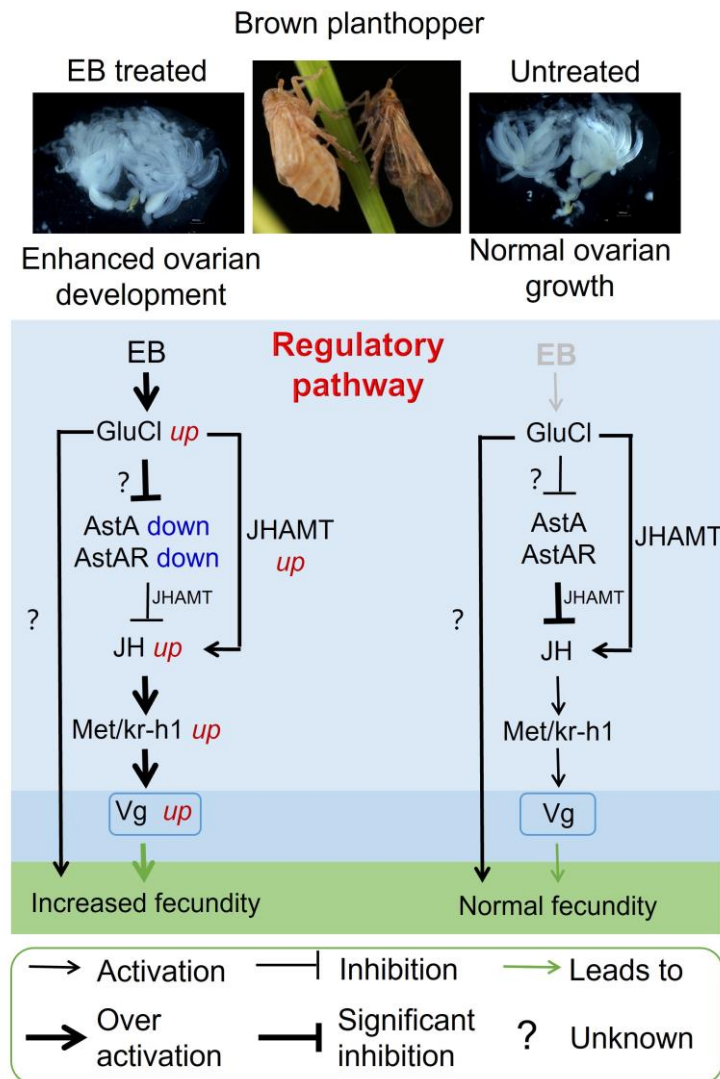
624 **Conclusion**

625 Our study has revealed a diverse suite of genes that act in combination to enhance
626 JH titer and thus fecundity following BPH exposure to EB. A schematic of how these
627 factors promote ovary development in the adult stage of *N. lugens* through the JH
628 signaling pathway is provided in Figure 6. Our findings provide the foundation for
629 further work to understand exactly how these genes interact and the mechanisms by

630 which their expression is activated or repressed by EB. Furthermore, our findings
631 provide fundamental insights into the molecular response in insects to xenobiotic
632 stress and illustrate that pesticides can have unexpected and negative impacts on pest
633 populations. In this regard our findings also have applied implications for the control of
634 a highly damaging crop pest. Previous studies have reported that avermectins such as
635 abamectin are toxic to the wolf spider *Pardosa pseudoannulata*, which is the main
636 predator of BPH in rice crops [78, 79]. Thus, these insecticides both stimulate
637 reproduction in BPH while killing their natural enemies providing a 'perfect storm' for
638 damaging BPH outbreaks. Based on these findings, to avoid BPH resurgence, we
639 suggest that the GluCl_s, EB and abamectin, should not be (or rarely be) applied to rice
640 plants at growth stages when BPHs are present. On a more optimistic note, our
641 findings have identified numerous genes that play key roles in BPH reproduction and
642 thus represent promising targets for the development of novel controls against this
643 important pest.

644

645 **Figure 6**



646

647 **Figure 6. Schematic of the proposed regulatory pathway of EB-enhanced fecundity**

648 **in BPH.** Enamectin benzoate (EB) exposure results in the upregulation of genes that promote

649 JH production (*JHAMT*, *Met* and *Kr-h1*) and the downregulation of genes that inhibit it

650 (allatostatin, *AstA* and allatostatin A receptor, *AstAR*). This transcriptome reprogramming is

651 dependent on the action of EB on its molecular target the glutamate-gated chloride channel

652 (*GluCl*) receptor. The resulting increased JH titer promotes *vg* synthesis and increased

653 fecundity in EB exposed insects. We observe significant cross-talk in the expression of genes

654 that inhibit JH production and those that promote it, with *AstAR* inhibiting the expression of

655 *JHAMT*, *Met* and *Kr-h1* and *GluCl* activating the expression of *JHAMT* which is responsible for

656 JH synthesis, and the JH signalling downstream genes *Met* and *Kr-h1*.

657 **Materials and methods**

658 **Insects**

659 BPH was initially collected from Wanan, JiangXi Province in 2020, reared on
660 'Taichung Native 1' (TN1) rice seedlings in the laboratory without exposure to any
661 insecticides. The strain was maintained in a climatic chamber at $27 \pm 1^\circ\text{C}$, with relative
662 humidity of $70 \pm 10\%$ and a light: dark = 16 h: 8 h photoperiod.

663 **Chemicals**

664 Emamectin benzoate (95.2%) was obtained from Hebei Weiyuan Co., Ltd. (Hebei,
665 China). Abamectin (96.8%) was obtained from Hebei Weiyuan Co., Ltd. (Hebei, China).
666 Pyriproxyfen (98%) was obtained from Shanghai Shengnong Co., Ltd. (Shanghai,
667 China). Methoprene (S)-(+)(mx7457-100mg) was purchased from Shanghai MaoKang
668 Biotechnology Co., Ltd., (Shanghai, China). Juvenile hormone standard sample
669 (J912305-10mg) was purchased from Shanghai Macklin Biotechnology Co., Ltd.,
670 (Shanghai, China).

671 **Bioassay**

672 Different life stages of insects were used to perform bioassay to investigate the
673 effects of insecticide on nymphs and adults. To test whether treatment of the nymph
674 stage of insects would promote reproduction in female, we used 4th instar nymphs of
675 BPH or 3rd instar nymph of *Laodelphax striatellus* and *Sogatella furcifera* to perform
676 bioassays. To test whether treatment of the adult stage of insects would promote
677 reproduction in female, we used newly emerged male and female BPH.

678 **Systemic route:** The rice-seeding dipping bioassay method was used to evaluate

679 the susceptibility of BPH, *L. striatellus* and *S. furcifera* to EB. Technical-grade
680 insecticides were dissolved in acetone as stock solution then diluted in a series of six
681 concentrations with water containing 0.1% Triton. Selected rice seedlings at the 6-8
682 cm growth stage were dipped in insecticide solutions for 30 s and then air-dried at
683 room temperature. The roots of the rice seedlings were wrapped with cotton strips and
684 placed seedlings placed in a plastic cup 5 cm in diameter. Fifteen insects were
685 introduced into each plastic cup for each replicate. The top of the cup was then sealed
686 with gauze to prevent escape. All experiments comprised at least three biological
687 replicates. Control rice seedlings were treated with 0.1% Triton X-100 water solution
688 only. All treatments were maintained under standard conditions of 27 ± 1 °C and 70–
689 80% relative humidity with a 16 h light/8 h dark photoperiod. Mortality was assessed
690 after 4 d for *N. lugens* or 2 d for *L. striatellus* and *S. furcifera* after treatment with
691 insecticides. The insects were considered dead if they were unable to move after a
692 gentle prodding with a fine brush.

693 For *Drosophila* larvae bioassay, we adopted a method described previously in our
694 lab with minor modifications [80]. Briefly, twenty third instar larvae were placed in fly
695 vials containing fly food (based on corn powder, brown sugar, yeast and agar)
696 supplemented with EB of different concentrations. Four concentrations (LC₁₀, LC₃₀ and
697 LC₅₀) were tested together with a negative (no insecticide) control. For *Drosophila* adult
698 bioassays, we selected virgin females three days after eclosion. Several
699 concentrations were overlaid onto fly food in standard *Drosophila* vials and allowed to
700 dry overnight at room temperature. 15 adult flies (three days after eclosion) were then

701 added to each vial and mortality assessed after 2 d. Four replicates were carried out
702 for each concentration. Control mortality was assessed using vials containing food with
703 solvent minus insecticide.

704 **Contact route:** For topical bioassays working insecticide solutions were prepared
705 in acetone. 4th instar nymphs or newly emerged males/females were anesthetized with
706 carbon dioxide for 5 s, and then 0.04 µl/insect test solution applied topically to the
707 dorsal plates with a capillary micro-applicator [26]. Insects were then placed in an
708 artificial climate incubator with a temperature of 27±1°C, a photoperiod of 16:8 h (L:D),
709 and a humidity of 70%±10%. Mortality was determined 2 d after treatment. Data with
710 over 20% mortality in the control treatment were discarded, and the assay was
711 repeated at least three times.

712 **Fecundity assays**

713 Fourth instar nymphs of BPH and 3rd instar nymph of *L. striatellus* and *S. furcifera*
714 were treated with the LC₁₅ and LC₅₀ of EB, and then transferred to fresh rice seedlings.
715 After eclosion, the adults were used in the following experiment. Newly emerged
716 treated adults and untreated adults were paired to produce four groups: untreated
717 males and untreated females (♂ck×♀ck; ck indicates untreated); untreated males and
718 treated females (♂ck×♀t; t indicates insecticide treated); treated males and untreated
719 females (♂t×♀ck); treated males and treated females (♂t×♀t). Each group comprised
720 at least 10 mating pairs. All pairs were transferred to glass cylinders (diameter 5 cm
721 and height 20 cm) containing rice plants (25 days old almost 20 cm high) as a food
722 source for eleven days. The number of eggs and nymphs in plants were counted by a

723 microscope.

724 For *Drosophila* egg-laying assay, we adopted our previous method [81]. Briefly,
725 insecticide-treated virgin females were paired with untreated males for three days and
726 then the mated females transferred into the *Drosophila* ovipositing apparatus. The
727 number of eggs were counted after 16 hours.

728 **Fitness analysis**

729 The fitness of EB-treated BPH were analyzed using methods reported previously
730 [10]. We selected two groups, ($\text{♂ck} \times \text{♀ck}$) and ($\text{♂ck} \times \text{♀t}$), to study the effects of the LC₅₀
731 concentration of EB on BPH fitness. In the case of systemic exposure, 4th instar
732 nymphs of BPH were treated with the LC₅₀ of EB for 4 days and then transferred to
733 tubes containing untreated rice plants for individual rearing. The rice plants were
734 replaced every three days with untreated plants. The emergence ratio, female ratio,
735 preoviposition period, female longevity, brachypterism female ratio and female weight
736 were calculated.

737 **Examination of ovary development**

738 Adult females from $\text{♂ck} \times \text{♀ck}$ control and $\text{♂ck} \times \text{♀t}$ group on 1, 3, 5, 7 DAE were
739 dissected for observe the ovary development. The detained eggs in ovary were
740 photographed and recorded. Each group has at least fifteen replicates.

741 To examination whether EB treated impairs egg maturation, we dissected
742 untreated or EB-treated ovaries and fixed them in 4% paraformaldehyde (PFA) in
743 phosphate buffered saline (PBS) for 30 min at room temperature. After four washes of

744 10 min (4 × 10 min) in PAT3 (PBS with 0.5% Triton X-100 and 0.5% bovine serum
745 albumin), the ovaries were then incubated with DAPI (4',6-diamidino-2-phenylindole,
746 100 nM) and Actin-stain 670 Fluorescent Phalloidin (200 nM). Imaging was performed
747 using Zeiss LSM980 confocal laser microscope.

748 **Measurements of glycogen, triglyceride, total protein content, cholesterol and** 749 **four sugars**

750 The content of glycogen, triglyceride, cholesterol and total protein was
751 determined by spectrophotometry at 620 nm, 510 nm, 510 nm and 562 nm
752 respectively using the glycogen assay kit (A043-1-1), triglyceride reagent kit (A110-1-
753 1), cholesterol assay kit (A111-1-1) and total protein assay kit (A045-2-2) obtained
754 from Nanjing Jiancheng Bioengineering Institute following to the manufacturer's
755 instructions. The determined results were normalized to the protein content in the
756 sample, which was determined using BCA Protein Assay Reagent Kit (Thermo
757 Scientific, Waltham, USA). Each sample contained tissue extracts from five adult
758 female BPH, with three biological replicates per sample.

759 To assess the content of four sugars (sucrose, glucose, fructose and trehalose)
760 in the extract of BPH tissue, the same extraction method was used as above. Sugar
761 content was quantified using the colorimetric method by scanning at 290 nm, 505
762 nm, 285 nm and 620 nm respectively using the sucrose reagent kit (A099-1-1),
763 glucose reagent kit (F006-1-1), fructose reagent kit (A085-1-1) and trehalose reagent
764 kit (A150-1-1) obtained from Nanjing Jiancheng Bioengineering Institute based on the
765 manufacturer's instructions. Each sample contained tissue extracts from five adult

766 female *N. lugens*, with three biological replicates per sample.

767 **Determination of Juvenile hormone III and ecdysone titers of BPH by ELISA**

768 The titer of Juvenile hormone III in BPH was measured using the Juvenile
769 hormone ELISA Kit (Lot Number: HLE92086, Shanghai HaLing Biotechnology Co., Ltd.,
770 Shanghai, China) which employs the dual-antibody sandwich ELISA method. The titer
771 of ecdysone in BPH were measured using the ecdysone ELISA Kit (Lot Number:
772 ZK14705, Shanghai ZhenKe Biotechnology Co., Ltd., Shanghai, China). At least three
773 biological replicates were employed for each treatment.

774 **Determination of Juvenile hormone III titer in BPH using HPLC-MS/MS**

775 The whole bodies of 5 individuals BPH were mixed with 1 ml of n-hexane, followed
776 by centrifugation at 10,000×g for 10 min, the upper hexane layer was then dried with
777 nitrogen, dissolved in methanol and sonicated for 10 min, after centrifugation at
778 10000×g for 10 min, the supernatant was collected through the organic filter membrane
779 of 0.22 μm into 2 ml vials for JH III determination. JH III standard sample (J912305-
780 10 mg) purchased from (Shanghai McLean Biochemical Technology Co. Ltd),
781 dissolved in methyl alcohol as stock solution 10,000 mg/L was diluted in a series of six
782 concentration gradients to serve as a reference. Liquid chromatography-tandem mass
783 spectrometry (LC-MS/MS) was then carried out using UPLC Xevo TQ-S Micro (Waters
784 technology), quantitative method according to the external standard, the
785 chromatographic column was EC-C18 (4.6 mm×150 mm, 2.7 μm), column temperature
786 was 30°C, injection volume was 20 μl, elution flow rate was 0.3 ml/min, and the mobile

787 phase was acetonitrile:formic acid water (90:10), detection wavelength was 218 nm,
788 the peak height was used for quantification.

789 **Cloning, sequence and phylogenetic analysis**

790 The NCBI database and BLAST program were used to carry out sequence
791 alignment and analysis. Open Reading Frames (ORFs) were predicted with EditSeq.
792 Primers were designed using the primer design tool in NCBI. Total RNA Extraction was
793 extracted from 30 adults BPH using TRIzol reagent (Invitrogen, Carlsbad, CA, USA)
794 according to the manufacturer's instructions. cDNA was synthesized using the Biotech
795 M-MLV reverse transcription kit. Full-length gene sequences were amplified by PCR
796 using cDNA as template and Rapid Taq Master Mix (Vazyme Biotech, Cat# P222-02).
797 The PCR product was purified on a 1% agarose gel, cloned into pClone007 Simple
798 Vector Kit (Tsingke Biotech, Cat# TSV-007S), and then sequenced using the 3730 XL
799 DNA analyzer (Applied Biosystems, Carlsbad, CA, USA). [Table S2](#) contains a list of
800 the primers used in this study.

801 The exon and intron architectures of AT, AstA, AstB, AstCC and AstACCC were
802 predicted based on the alignments of putative ORFs against their corresponding
803 genomic sequences. Sequence similarity/annotations and orthologous gene searches
804 were performed using BLAST programs available in NCBI. Multiple alignments of the
805 complete amino acid sequences were performed with Clustal Omega
806 (<http://www.ebi.ac.uk/Tools/msa/clustalo>). Phylogeny was conducted using the
807 maximum likelihood technique to create phylogenetic trees and these were

808 bootstrapped with 1000 replications were used using the MEGA 6 software [82].

809 RNA interference

810 Double-stranded RNA (dsRNA) of *gfp* (green fluorescent protein), *JHAMT*
811 (juvenile hormone acid O-methyltransferase), *Met* (methoprene-tolerant), *Kr-h1*
812 (krüppel homolog 1), *AstAR* (allatostatin-A receptor) and *GluCl* (glutamate-gated
813 chloride channel) was prepared using Ambion's MEGAscript T7 kit instructions
814 following the manufacturer's instructions. The primer sequences for double-stranded
815 RNA synthesis are listed in Table S2. Newly emerged females were injected with 40
816 nl (5,000 ng/μl) of double-stranded RNA of *gfp* (*dsgfp*) or double-stranded RNA of the
817 target genes in the conjunctive part between prothorax and mesothorax of insects. In
818 the RNAi experiments, BPH were then treated with the LC₅₀ of EB 24h after dsRNA
819 injection and the whole body sampled for qRT-PCR analysis.

820 Quantitative RT-PCR

821 Fourth instar nymphs of BPH were treated with EB after which total RNA was
822 extracted from 5th instar nymphs and 1-7 day post-eclosion females of *N. lugens* using
823 the methods detailed above. The HiScript® II RT SuperMix for qPCR (+gDNA wiper)
824 kit from Vazyme, Nanjing, China, was used to create first-strand cDNA. Primer3
825 (<http://bioinfo.ut.ee/primer3/>) was used to design real-time quantitative PCR (qPCR)
826 primers listed in Table S2. mRNA levels of candidate genes were detected by qPCR
827 using the UltraSYBR Mixture (with ROX) Kit (CW BIO, Beijing, China). Each reaction
828 contained 2 μL of cDNA template (500 ng), 1 μL each forward and reverse qPCR primer

829 (10 μ M), 10 μ L of UltraSYBR mixture buffer, and 6 μ L of RNase-free water. Q-PCR
830 was run on an ABI 7500 Real-Time PCR System (Applied Biosystems, Foster City, CA)
831 under the following conditions: 5 min at 95°C, followed by 40 cycles of 95°C for 10 s
832 and 60°C for 30 s. Three independent biological replicates and four technical replicates
833 were used in each qPCR experiment. The housekeeping genes 18S ribosomal RNA
834 of BPH were selected to normalize the expression of candidate genes. The $2^{-\Delta\Delta C_t}$
835 method (Ct represents the cycle threshold) was used to measure relative expression
836 levels [83]. Three biological replicates were used for statistical comparison between
837 samples. Table S2 contains a list of the primers used in this study.

838 **Statistics**

839 PoloPlus v2.0 (LeOra Software 2008) was used to calculate the lethal
840 concentration (LC₅₀) and 95% fiducial limits (95% F.L.). GraphPad Prism 8.0 software
841 (GraphPad Software Inc., San Diego, USA) was used to generate graphs and perform
842 statistical analysis of data. Data presented in this study were first verified for normal
843 distribution using the D'Agostino–Pearson normality test. One-way analysis of
844 variance (ANOVA) with Duncan's multiple range test was used to test differences
845 among multiple groups of normally distributed groups of data. Student's t test was used
846 to test the differences between two groups. If not normally distributed, Mann–Whitney
847 test was used for pairwise comparisons, and Kruskal–Wallis test was used for
848 comparisons among multiple groups, followed by Dunn's multiple comparisons. All
849 data are presented as mean \pm s.e.m. The sample sizes and statistical tests used for
850 each experiment are stated in the figures or figure legends.

Table S2 Sequences of oligonucleotide primers used in this study.

Primers	Primer sequences (5' - 3')
For cDNA cloning	
Allatotropin:	
NIAT-F	TACGCGGCCAAACACACTTA
NIAT-R	AGGGAAAGAGGGCGAAATTCA
Allatostatins:	
NIastA-F	TCGGCCGTCACAAGTCAAG
NIastA-R	CCGAACCCGTACTIONCATGCT
NIastB-F	ACCGGGCTCACAGGAATTTT
NIastB-R	TGTAGGCGCAGATCTTGAGG
NIastCC-F	AACACAGCTCTACGAGGCAC
NIastCC-R	CCAAGCAGGTGACTGCCATA
NIastCCC-F	TTTGTGTGTGCTTGCAGGTG
NIastCCC-R	GGATAGAAACGGTAGATTTGGTAGA
Allatostatins receptor:	
NIA16-F	CCTCATTGTGGAACCACCGA
NIA16-R	CGCAGCTGTAAGGTGGAAGA
NIA2-F	GAACGTAATGGGAGTCGGCA
NIA2-R	GTTTTTGTGAGCGCCGACTT
NIA10-F	ATGCAAACACGGCCAGCCT
NIA10-R	TTAATCGTCTCTGCTCAACTCCAAAGGAAGGT
NIA1-F	CGACCAGACCACTCTACTGC
NIA1-R	ACGTGGACCTCACTATACCAAAAA
For Quantitative RT-PCR	
Q-NI18S-F	CGCTACTACCGATTGAA
Q-NI18S-R	GGAAACCTTGTTACGACTT
Q-vitellogenin-F	GTGGCTCGTTCAAGTTATGG
Q-vitellogenin-R	GCAATCTCTGGGTGCTGTTG
Q-Vitellogenin receptor-F	AGGCAGCCACACAGATAACCGC
Q-Vitellogenin receptor-R	AGCCGCTCGCTCCAGAACATT
Q-JHE-F	GAGCCTCACATCCACAGC
Q-JHE-R	AATGGGAGCCCTACGC
Q-NIMet-F	GGTGGTAAACGGATTGGAAA
Q-NIMet-R	CATCGTCAGCCAACCTCGATA
Q-NIFAMet-F	GCAAAGTCAGCAATCCGCAAGAAC
Q-NIFAMet-R	ACACCGTAGTGGGTGACAACGAATG
Q-JHAMT-F	GAACCTGCAGGCCAAACACA
Q-JHAMT-R	ACCACTCGGTTGGGCTGAAT
Q-NIKr-h1-F	TGATGAGGCACACGATGACT
Q-NIKr-h1-R	ATGGAAGGCCACATCAAGAG
Q-NIAT-F	CACGATACGTGGCTTCAAGA
Q-NIAT-R	ACGATCACTTTGCGCCAATTC
Q-NIastA-F	AGGACTTACTGGGCGAGGAT

Q-NIAstA-R	GGTGTCTCGTTTCCTGGTGT
Q-NIAstB-F	AGCGAGCTAGACGAGGACAA
Q-NIAstB-R	TCGTCTCTGCTCAACTCCAA
Q-NIAstCC-F	CTGCTCCCAGTGAAAAGGAG
Q-NIAstCC-R	GCTTCCAGTAACTGCGCTTC
Q-NIAstCCC-F	TGTGCTTGCAGGTGGTAGTC
Q-NIAstCCC-R	AGAAGCATGTGACTGCGTTG
Q-NIA2-F	TCCTGGTGCTGAAGAGTGTG
Q-NIA2-R	CTTTTCGGGCCCATTAATTT
Q-NLA1-F	ATATCGGCACCGAAGATGAG
Q-NLA1-R	GTCTGACCCGACAGGTTCTC
Q-NLA10-F	ACTGGGTGTCGACCAATCTC
Q-NLA10-R	TCGGTAGCGAGGAAGACAGT
Q-NLA16-F	TACCGTTCTGTGGGATGTCA
Q-NLA16-R	CCGGGATATCAAAGACGAGA
Q-NIGluCI-F	CACTGACTGAGGCCAACAGA
Q-NIGluCI-R	GCTGGCCATTCTTAGTGAGC

For double-stranded RNA synthesis

T7-EGFP-F	TAATACGACTCACTATAGGGCGTAAACGGCCACAAGTTCA
T7-EGFP-R	TAATACGACTCACTATAGGGGACTGGGTGCTCAGGTAGTG
T7-Kr-h1-F	TAATACGACTCACTATAGGGCGCCAGTGAAAGTGAGACCT
T7-Kr-h1-R	TAATACGACTCACTATAGGGGAGACCGCAAGTGGTTCTGA
T7-Met-F	TAATACGACTCACTATAGGGCCACCAACCAGCAGATGAACCTGA
T7-Met-R	TAATACGACTCACTATAGGGCCACGCAAAGCCTCGTACTCTTGG
T7-JHAMT-F	TAATACGACTCACTATAGGGCTCCAGGCCATTGTCCCTCA
T7-JHAMT-R	TAATACGACTCACTATAGGGTTGGCCTGCAGGTTCTTTGG
T7-AstA-R-F	TAATACGACTCACTATAGGGTACTGCCGTTCTGGCCTTTT
T7-AstA-R-R	TAATACGACTCACTATAGGGGTGATCTGGAAGAGCGGCTT
T7-Glucl-F	TAATACGACTCACTATAGGGACACATCACCTGCTCACCTG
T7-Glucl-R	TAATACGACTCACTATAGGGGTGTGTTTGCCTGCTGTCTG

853 **Acknowledgments**

854 This research was funded by the National Key R&D Program of China

855 (2022YFD1700200) and National Natural Science Foundation of China (32022011).

856

857 References

- 858 1. Janssen A, van Rijn PCJ. Pesticides do not significantly reduce arthropod pest densities in the presence of natural enemies. *Ecol Lett.*
859 2021;24(9):2010-24. doi: <https://doi.org/10.1111/ele.13819>.
- 860 2. Wu SF, Zeng B, Zheng C, Mu XC, Zhang Y, Hu J, et al. The evolution of insecticide resistance in the brown planthopper (*Nilaparvata*
861 *lugens* Stål) of China in the period 2012–2016. *Sci Rep.* 2018;8(1):4586. doi: 10.1038/s41598-018-22906-5.
- 862 3. Wu J, Ge L, Liu F, Song Q, Stanley D. Pesticide-induced planthopper population resurgence in rice cropping systems. *Annu Rev Entomol.*
863 2020;65(1):409-29. doi: 10.1146/annurev-ento-011019-025215. PubMed PMID: 31610135.
- 864 4. Guedes RNC, Smagghe G, Stark JD, Desneux N. Pesticide-induced stress in arthropod pests for optimized integrated pest management
865 programs. *Annu Rev Entomol.* 2016;61(1):43-62. doi: 10.1146/annurev-ento-010715-023646.
- 866 5. Hardin MR, Benrey B, Coll M, Lamp WO, Roderick GK, Barbosa P. Arthropod pest resurgence: an overview of potential mechanisms.
867 *Crop Protection.* 1995;14(1):3-18. doi: [https://doi.org/10.1016/0261-2194\(95\)91106-P](https://doi.org/10.1016/0261-2194(95)91106-P).
- 868 6. Ge L-Q, Wu J-C, Zhao K-F, Chen Y, Yang G-Q. Induction of Nlvg and suppression of Nljhe gene expression in *Nilaparvata lugens* (Stål)
869 (Hemiptera: Delphacidae) adult females and males exposed to two insecticides. *Pestic Biochem Physiol* 2010;98(2):269-78. doi:
870 <https://doi.org/10.1016/j.pestbp.2010.06.018>.
- 871 7. Zhang Y-X, Zhu Z-F, Lu X-L, Li X, Ge L-Q, Fang J-C, et al. Effects of two pesticides, TZP and JGM, on reproduction of three planthopper
872 species, *Nilaparvata lugens* Stål, *Sogatella furcifera* Horvath, and *Laodelphax striatella* Fallén. *Pestic Biochem Physiol* 2014;115:53-7. doi:
873 <https://doi.org/10.1016/j.pestbp.2014.07.012>.
- 874 8. Wu Y, Ding J, Xu B, You L, Ge L, Yang G, et al. Two fungicides alter reproduction of the small brown planthopper *Laodelphax striatellus*
875 by influencing gene and protein expression. *J Proteome Res.* 2018;17(3):978-86. doi: 10.1021/acs.jproteome.7b00612.
- 876 9. Sōgawa K. The rice brown planthopper: Feeding physiology and host plant interactions. *Annu Rev Entomol.* 1982;27(1):49-73. doi:
877 10.1146/annurev.en.27.010182.000405.
- 878 10. Zeng B, Chen F-R, Liu Y-T, Di G, Zhang Y-J, Feng Z-R, et al. A chitin synthase mutation confers widespread resistance to buprofezin, a
879 chitin synthesis inhibitor, in the brown planthopper, *Nilaparvata lugens*. *J Pest Sci.* 2023;96:819–32. doi: 10.1007/s10340-022-01538-9.
- 880 11. Ishaaya I, Kontsedalov S, Horowitz AR. Emamectin, a novel insecticide for controlling field crop pests. *Pest Manag Sci.*
881 2002;58(11):1091-5. doi: <https://doi.org/10.1002/ps.535>.
- 882 12. Chintalapati P, Katti G, Puskur RR, Nagella Venkata K. Neonicotinoid-induced resurgence of rice leafhopper, *Cnaphalocrocis medinalis*
883 (Guénee). *Pest Manag Sci.* 2016;72(1):155-61. doi: 10.1002/ps.3983.
- 884 13. Zhang Y, Ruan Y, Gong C, Zhang S, Zhang J, He Y, et al. Reproductive outbreaks of *Sogatella furcifera* mediated by overexpression of the
885 nuclear receptor USP under pressure from triflumezopyrim. *Int J Mol Sci.* 2022;23(22):13769. PubMed PMID: doi:10.3390/ijms232213769.
- 886 14. Ge L-Q, Huang L-J, Yang G-Q, Song Q-S, Stanley D, Gurr GM, et al. Molecular basis for insecticide-enhanced thermotolerance in the
887 brown planthopper *Nilaparvata lugens* Stål (Hemiptera:Delphacidae). *Mol Ecol.* 2013;22(22):5624-34. doi: 10.1111/mec.12502.
- 888 15. Wang G, Vega-Rodríguez J, Diabate A, Liu J, Cui C, Nignan C, et al. Clock genes and environmental cues coordinate *Anopheles* pheromone
889 synthesis, swarming, and mating. *Science.* 2021;371(6527):411. doi: 10.1126/science.abd4359.
- 890 16. Meiselman MR, Alpert MH, Cui X, Shea J, Gregg I, Gallio M, et al. Recovery from cold-induced reproductive dormancy is regulated by
891 temperature-dependent AstC signaling. *Current Biol.* 2022;32(6):1362-75.e8. doi: <https://doi.org/10.1016/j.cub.2022.01.061>.
- 892 17. Roy S, Saha TT, Johnson L, Zhao B, Ha J, White KP, et al. Regulation of gene expression patterns in mosquito reproduction. *PLoS Genet.*
893 2015;11(8):e1005450. doi: 10.1371/journal.pgen.1005450.
- 894 18. Smykal V, Raikhel AS. Nutritional control of insect reproduction. *Curr Opin Insect Sci.* 2015;11:31-8. doi:
895 <https://doi.org/10.1016/j.cois.2015.08.003>.
- 896 19. Santos CG, Humann FC, Hartfelder K. Juvenile hormone signaling in insect oogenesis. *Curr Opin Insect Sci.* 2019;31:43-8. doi:
897 <https://doi.org/10.1016/j.cois.2018.07.010>.
- 898 20. Hun LV, Okamoto N, Imura E, Maxson R, Bittar R, Yamanaka N. Essential functions of mosquito ecdysone importers in development
899 and reproduction. *Proc Natl Acad Sci U S A.* 2022;119(25):e2202932119. doi: doi:10.1073/pnas.2202932119.

- 900 21. Ling L, Raikhel AS. Serotonin signaling regulates insulin-like peptides for growth, reproduction, and metabolism in the disease vector
901 *Aedes aegypti*. Proc Natl Acad Sci U S A. 2018;115(42):E9822. doi: 10.1073/pnas.1808243115.
- 902 22. Lu K, Chen X, Liu W-T, Zhou Q. TOR pathway-mediated juvenile hormone synthesis regulates nutrient-dependent female reproduction
903 in *Nilaparvata lugens* (Stål). Int J Mol Sci. 2016;17(4):438. PubMed PMID: doi:10.3390/ijms17040438.
- 904 23. Du B, Ding D, Ma C, Guo W, Kang L. Locust density shapes energy metabolism and oxidative stress resulting in divergence of flight
905 traits. Proc Natl Acad Sci U S A. 2022;119(1):e2115753118. doi: 10.1073/pnas.2115753118.
- 906 24. Ahmed TH, Saunders TR, Mullins D, Rahman MZ, Zhu J. Molecular action of pyriproxyfen: Role of the Methoprene-tolerant protein in
907 the pyriproxyfen-induced sterilization of adult female mosquitoes. PLoS Negl Trop Dis. 2020;14(8):e0008669. doi:
908 10.1371/journal.pntd.0008669.
- 909 25. Luo W, Liu S, Zhang W, Yang L, Huang J, Zhou S, et al. Juvenile hormone signaling promotes ovulation and maintains egg shape by
910 inducing expression of extracellular matrix genes. Proc Natl Acad Sci U S A. 2021;118(39):e2104461118. doi: 10.1073/pnas.2104461118.
- 911 26. Yao R, Zhao DD, Zhang S, Zhou LQ, Wang X, Gao CF, et al. Monitoring and mechanisms of insecticide resistance in *Chilo suppressalis*
912 (Lepidoptera: Crambidae), with special reference to diamides. Pest Manag Sci. 2017;73(6):1169-78. doi: 10.1002/ps.4439.
- 913 27. Jing Y-P, Wen X, Li L, Zhang S, Zhang C, Zhou S. The vitellogenin receptor functionality of the migratory locust depends on its
914 phosphorylation by juvenile hormone. Proc Natl Acad Sci U S A. 2021;118(37):e2106908118. doi: 10.1073/pnas.2106908118.
- 915 28. Ling L, Raikhel AS. Cross-talk of insulin-like peptides, juvenile hormone, and 20-hydroxyecdysone in regulation of metabolism in the
916 mosquito *Aedes aegypti*. Proc Natl Acad Sci U S A. 2021;118(6):e2023470118. doi: 10.1073/pnas.2023470118.
- 917 29. Zheng H, Wang N, Yun J, Xu H, Yang J, Zhou S. Juvenile hormone promotes paracellular transport of yolk proteins via remodeling zonula
918 adherens at tricellular junctions in the follicular epithelium. PLoS Genet. 2022;18(6):e1010292. doi: 10.1371/journal.pgen.1010292.
- 919 30. Guo W, Song J, Yang P, Chen X, Chen D, Ren D, et al. Juvenile hormone suppresses aggregation behavior through influencing antennal
920 gene expression in locusts. PLoS Genet. 2020;16(4):e1008762. doi: 10.1371/journal.pgen.1008762.
- 921 31. BOWNES M, REMBOLD H. The titre of juvenile hormone during the pupal and adult stages of the life cycle of *Drosophila melanogaster*.
922 Eur J Biochem. 1987;164(3):709-12. doi: <https://doi.org/10.1111/j.1432-1033.1987.tb11184.x>.
- 923 32. Gospocic J, Glastad KM, Sheng L, Shields EJ, Berger SL, Bonasio R. Kr-h1 maintains distinct caste-specific neurotranscriptomes in
924 response to socially regulated hormones. Cell. 2021;184(23):5807-23.e14. doi: <https://doi.org/10.1016/j.cell.2021.10.006>.
- 925 33. Nouzova M, Rivera-Pérez C, Noriega FG. Omics approaches to study juvenile hormone synthesis. Curr Opin Insect Sci. 2018;29:49-55.
926 doi: <https://doi.org/10.1016/j.cois.2018.05.013>.
- 927 34. Liu S, Zhang C, Yang B, Gu J, Liu Z. Cloning and characterization of a putative farnesoic acid O -methyltransferase gene from the brown
928 planthopper, *Nilaparvata lugens*. J Insect Sci. 2010;10(1). doi: 10.1673/031.010.10301.
- 929 35. Shinoda T, Itoyama K. Juvenile hormone acid methyltransferase: A key regulatory enzyme for insect metamorphosis. Proc Natl Acad
930 Sci U S A. 2003;100(21):11986. doi: 10.1073/pnas.2134232100.
- 931 36. Zhu G-H, Jiao Y, Chereddy SCRR, Noh MY, Palli SR. Knockout of juvenile hormone receptor, Methoprene-tolerant, induces black larval
932 phenotype in the yellow fever mosquito, *Aedes aegypti*. Proc Natl Acad Sci U S A. 2019;201905729. doi: 10.1073/pnas.1905729116.
- 933 37. Riddiford LM. Rhodnius, golden oil, and met: A history of juvenile hormone research. Front Cell Dev Biol. 2020;8(679). doi:
934 10.3389/fcell.2020.00679.
- 935 38. Jindra M, Palli SR, Riddiford LM. The juvenile hormone signaling pathway in insect development. Annu Rev Entomol. 2013;58(1):181-
936 204. doi: 10.1146/annurev-ento-120811-153700. PubMed PMID: 22994547.
- 937 39. Zhang C, Kim AJ, Rivera-Perez C, Noriega FG, Kim Y-J. The insect somatostatin pathway gates vitellogenesis progression during
938 reproductive maturation and the post-mating response. Nat Commun. 2022;13(1):969. doi: 10.1038/s41467-022-28592-2.
- 939 40. Shen Y, Chen Y-Z, Lou Y-H, Zhang C-X. Vitellogenin and vitellogenin-like genes in the brown planthopper. Front Physiol. 2019;10. doi:
940 10.3389/fphys.2019.01181.
- 941 41. Kamita SG, Hinton AC, Wheelock CE, Wogulis MD, Wilson DK, Wolf NM, et al. Juvenile hormone (JH) esterase: why are you so JH specific?
942 Insect Biochem Mol Biol. 2003;33(12):1261-73. doi: <https://doi.org/10.1016/j.ibmb.2003.08.004>.
- 943 42. Kataoka H, Toschi A, Li JP, Carney RL, Schooley DA, Kramer SJ. Identification of an allatotropin from adult *Manduca Sexta*. Science.

- 944 1989;243(4897):1481-3. doi: doi:10.1126/science.243.4897.1481.
- 945 43. Woodhead AP, Stay B, Seidel SL, Khan MA, Tobe SS. Primary structure of four allatostatins: neuropeptide inhibitors of juvenile hormone
946 synthesis. Proc Natl Acad Sci U S A. 1989;86(15):5997-6001. doi: doi:10.1073/pnas.86.15.5997.
- 947 44. Kramer SJ, Toschi A, Miller CA, Kataoka H, Quistad GB, Li JP, et al. Identification of an allatostatin from the tobacco hornworm *Manduca*
948 *sexta*. Proc Natl Acad Sci U S A. 1991;88(21):9458-62. doi: doi:10.1073/pnas.88.21.9458.
- 949 45. Lorenz MW, Kellner R, Hoffmann KH. A family of neuropeptides that inhibit juvenile hormone biosynthesis in the cricket, *Gryllus*
950 *bimaculatus*. J Biol Chem. 1995;270(36):21103-8. doi: 10.1074/jbc.270.36.21103.
- 951 46. Bellés X, Graham LA, Bendenab WG, Ding Q, Edwards JP, Weaver RJ, et al. The molecular evolution of the allatostatin precursor in
952 cockroaches. Peptides. 1999;20(1):11-22. doi: [https://doi.org/10.1016/S0196-9781\(98\)00155-7](https://doi.org/10.1016/S0196-9781(98)00155-7).
- 953 47. Stay B, Tobe SS. The role of allatostatins in juvenile hormone synthesis in insects and crustaceans. Annu Rev Entomol. 2007;52(1):277-
954 99. doi: 10.1146/annurev.ento.51.110104.151050. PubMed PMID: 16968202.
- 955 48. Wegener C, Chen J. Allatostatin A signalling: Progress and new challenges from a paradigmatic pleiotropic invertebrate neuropeptide
956 family. Front Physiol. 2022;13. doi: 10.3389/fphys.2022.920529.
- 957 49. Verlinden H, Gijbels M, Lismont E, Lenaerts C, Vanden Broeck J, Marchal E. The pleiotropic allatoregulatory neuropeptides and their
958 receptors: A mini-review. J Insect Physiol. 2015;80:2-14. doi: <https://doi.org/10.1016/j.jinsphys.2015.04.004>.
- 959 50. Yin G-L, Yang J-S, Cao J-X, Yang W-J. Molecular cloning and characterization of FGLamide allatostatin gene from the prawn,
960 *Macrobrachium rosenbergii*. Peptides. 2006;27(6):1241-50. doi: <https://doi.org/10.1016/j.peptides.2005.11.015>.
- 961 51. Wang C, Chin-Sang I, Bendena WG. The FGLamide-Allatostatins influence foraging behavior in *Drosophila melanogaster*. PLOS ONE.
962 2012;7(4):e36059. doi: 10.1371/journal.pone.0036059.
- 963 52. Veenstra JA. Allatostatin C and its paralog allatostatin double C: The arthropod somatostatins. Insect Biochem Mol Biol.
964 2009;39(3):161-70. doi: <https://doi.org/10.1016/j.ibmb.2008.10.014>.
- 965 53. Veenstra JA. Allatostatins C, double C and triple C, the result of a local gene triplication in an ancestral arthropod. Gen Comp Endocrinol.
966 2016;230-231:153-7. doi: <https://doi.org/10.1016/j.ygcen.2016.04.013>.
- 967 54. Nässel DR. Neuropeptides in the nervous system of *Drosophila* and other insects: multiple roles as neuromodulators and
968 neurohormones. Prog Neurobiol. 2002;68(1):1-84. doi: [https://doi.org/10.1016/S0301-0082\(02\)00057-6](https://doi.org/10.1016/S0301-0082(02)00057-6).
- 969 55. Tanaka Y, Suetsugu Y, Yamamoto K, Noda H, Shinoda T. Transcriptome analysis of neuropeptides and G-protein coupled receptors
970 (GPCRs) for neuropeptides in the brown planthopper *Nilaparvata lugens*. Peptides. 2014;53:125-33. doi:
971 <https://doi.org/10.1016/j.peptides.2013.07.027>.
- 972 56. Audsley N, Vandersmissen HP, Weaver R, Dani P, Matthews J, Down R, et al. Characterisation and tissue distribution of the PISCF
973 allatostatin receptor in the red flour beetle, *Tribolium castaneum*. Insect Biochem Mol Biol. 2013;43(1):65-74. doi:
974 <https://doi.org/10.1016/j.ibmb.2012.09.007>.
- 975 57. Sparks TC, Storer N, Porter A, Slater R, Nauen R. Insecticide resistance management and industry: the origins and evolution of the
976 Insecticide Resistance Action Committee (IRAC) and the mode of action classification scheme. Pest Manag Sci. 2021;77(6):2609-19. doi:
977 <https://doi.org/10.1002/ps.6254>.
- 978 58. Sparks TC, Crossthwaite AJ, Nauen R, Banba S, Cordova D, Earley F, et al. Insecticides, biologics and nematicides: Updates to IRAC's
979 mode of action classification - a tool for resistance management. Pestic Biochem Physiol 2020;167:104587. doi:
980 <https://doi.org/10.1016/j.pestbp.2020.104587>.
- 981 59. Wu SF, Mu XC, Dong YX, Wang LX, Wei Q, Gao CF. Expression pattern and pharmacological characterisation of two novel alternative
982 splice variants of the glutamate-gated chloride channel in the small brown planthopper *Laodelphax striatellus*. Pest Manag Sci.
983 2017;73(3):590-7. doi: 10.1002/ps.4340.
- 984 60. Wang L-P, Shen J, Ge L-Q, Wu J-C, Yang G-Q, Jahn GC. Insecticide-induced increase in the protein content of male accessory glands and
985 its effect on the fecundity of females in the brown planthopper *Nilaparvata lugens* Stål (Hemiptera: Delphacidae). Crop Protection.
986 2010;29(11):1280-5. doi: <https://doi.org/10.1016/j.cropro.2010.07.009>.
- 987 61. Ge L-Q, Cheng Y, Wu J-C, Jahn GC. Proteomic analysis of insecticide triazophos-induced mating-responsive proteins of *Nilaparvata*

- 988 *lugens* Stål (Hemiptera: Delphacidae). J Proteome Res. 2011;10(10):4597-612. doi: 10.1021/pr200414g.
- 989 62. Zhao K-F, Shi Z-P, Wu J-C. Insecticide-induced enhancement of flight capacity of the brown planthopper *Nilaparvata lugens* Stål
990 (Hemiptera: Delphacidae). Crop Protection. 2011;30(4):476-82. doi: <https://doi.org/10.1016/j.cropro.2010.11.026>.
- 991 63. Wan D-J, Chen J, Jiang L-B, Ge L-Q, Wu J-C. Effects of the insecticide triazophos on the ultrastructure of the flight muscle of the brown
992 planthopper *Nilaparvata lugens* Stål (Hemiptera: Delphacidae). Crop Protection. 2013;43:54-9. doi:
993 <https://doi.org/10.1016/j.cropro.2012.08.011>.
- 994 64. Cheng J, Huang L-J, Zhu Z-F, Jiang L-B, Ge L-Q, Wu J-C. Heat-dependent fecundity enhancement observed in *Nilaparvata lugens*
995 (Hemiptera: Delphacidae) after treatment with triazophos. Environ Entomol. 2014;43(2):474-81. doi: 10.1603/en13249.
- 996 65. Yang H, Zhou C, Jin D-c, Gong M-f, Wang Z, Long G-y. Sublethal effects of abamectin on the development, fecundity, and wing morphs
997 of the brown planthopper *Nilaparvata lugens*. J Asia Pac Entomol. 2019;22(4):1180-6. doi: <https://doi.org/10.1016/j.aspen.2019.10.012>.
- 998 66. Yin J-L, Xu H-W, Wu J-C, Hu J-H, Yang G-Q. Cultivar and insecticide applications affect the physiological development of the brown
999 planthopper, *Nilaparvata lugens* (Stål) (Hemiptera: Delphacidae). Environ Entomol. 2014;37(1):206-12. doi: 10.1603/0046-
1000 225x(2008)37[206:caiaat]2.0.co;2.
- 1001 67. Riddiford LM. Juvenile hormone action: A 2007 perspective. J Insect Physiol. 2008;54(6):895-901. doi:
1002 <https://doi.org/10.1016/j.jinsphys.2008.01.014>.
- 1003 68. Xu B, You L-L, Wu Y, Ding J, Ge L-Q, Wu J-C. Transmission electron microscopy (TEM) observations of female oocytes from *Nilaparvata*
1004 *lugens* (Hemiptera: Delphacidae): Antibiotic jinggangmycin (JGM)-induced stimulation of reproduction and associated changes in hormone
1005 levels. J Econ Entomol. 2016;109(4):1677-82. doi: 10.1093/jee/tow085.
- 1006 69. Shah S, Zhang S-S, Elgizawy KK, Yan W-H, Tang N, Wu G, et al. Diallyl trisulfide reduced the reproductive capacity of male *Sitotroga*
1007 *cerealella* via the regulation of juvenile and ecdysone hormones. Ecotoxicol Environ Saf. 2022;248:114304. doi:
1008 <https://doi.org/10.1016/j.ecoenv.2022.114304>.
- 1009 70. Jin M-n, Xue J, Yao Y, Lin X-d. Molecular characterization and functional analysis of krüppel-homolog 1 (Kr-h1) in the brown
1010 planthopper, *Nilaparvata lugens* (Stål). J Integr Agric. 2014;13(9):1972-81. doi: [https://doi.org/10.1016/S2095-3119\(13\)60654-1](https://doi.org/10.1016/S2095-3119(13)60654-1).
- 1011 71. Lin X, Yao Y, Wang B. Methoprene-tolerant (Met) and Krüppel-homologue 1 (Kr-h1) are required for ovariole development and egg
1012 maturation in the brown plant hopper. Sci Rep. 2015;5(1):18064. doi: 10.1038/srep18064.
- 1013 72. Zhang C, Daubnerova I, Jang Y-H, Kondo S, Žitňan D, Kim Y-J. The neuropeptide allatostatin C from clock-associated DN1p neurons
1014 generates the circadian rhythm for oogenesis. Proc Natl Acad Sci U S A. 2021;118(4):e2016878118. doi: 10.1073/pnas.2016878118.
- 1015 73. Stay B, Fairbairn S, Yu CG. Role of allatostatins in the regulation of juvenile hormone synthesis. Arch Insect Biochem Physiol.
1016 1996;32(3-4):287-97. doi: [https://doi.org/10.1002/\(SICI\)1520-6327\(1996\)32:3/4<287::AID-ARCH3>3.0.CO;2-Q](https://doi.org/10.1002/(SICI)1520-6327(1996)32:3/4<287::AID-ARCH3>3.0.CO;2-Q).
- 1017 74. Yagi KJ, Kwok R, Chan KK, Setter RR, Myles TG, Tobe SS, et al. Phe-Gly-Leu-amide allatostatin in the termite *Reticulitermes flavipes*:
1018 Content in brain and corpus allatum and effect on juvenile hormone synthesis. J Insect Physiol. 2005;51(4):357-65. doi:
1019 <https://doi.org/10.1016/j.jinsphys.2004.12.006>.
- 1020 75. Hentze JL, Carlsson MA, Kondo S, Nässel DR, Rewitz KF. The neuropeptide allatostatin A regulates metabolism and feeding decisions
1021 in *Drosophila*. Sci Rep. 2015;5(1):11680. doi: 10.1038/srep11680.
- 1022 76. Liu H-P, Lin S-C, Lin C-Y, Yeh S-R, Chiang A-S. Glutamate-gated chloride channels inhibit juvenile hormone biosynthesis in the cockroach,
1023 *Diploptera punctata*. Insect Biochem Mol Biol. 2005;35(11):1260-8. doi: <http://dx.doi.org/10.1016/j.ibmb.2005.06.004>.
- 1024 77. Hasebe M, Shiga S. Clock gene-dependent glutamate dynamics in the bean bug brain regulate photoperiodic reproduction. PLOS Biol.
1025 2022;20(9):e3001734. doi: 10.1371/journal.pbio.3001734.
- 1026 78. Chen B, Wen L, Zhao J, Liang H, Jiao X. Laboratory risk assessment of seven insecticides to the wolf spider *Pardosa pseudoannulata*. J
1027 Plant Protect. 2017;44:1059-60.
- 1028 79. Sogawa K. Planthopper outbreaks in different paddy ecosystems in Asia: Man-made hopper plagues that threatened the green
1029 revolution in rice. In: Heong KL, Cheng J, Escalada MM, editors. Rice Planthoppers: Ecology, Management, Socio Economics and Policy.
1030 Dordrecht: Springer Netherlands; 2015. p. 33-63.
- 1031 80. Huang JM, Rao C, Wang S, He LF, Zhao SQ, Zhou LQ, et al. Multiple target-site mutations occurring in lepidopterans confer resistance

- 1032 to diamide insecticides. *Insect Biochem Mol Biol.* 2020;121:103367. doi: <https://doi.org/10.1016/j.ibmb.2020.103367>.
- 1033 81. Wu SF, Ja YL, Zhang YJ, Yang CH. Sweet neurons inhibit texture discrimination by signaling TMC-expressing mechanosensitive neurons
- 1034 in *Drosophila*. *eLife.* 2019;8:e46165. doi: 10.7554/eLife.46165.
- 1035 82. Tamura K, Stecher G, Peterson D, Filipski A, Kumar S. MEGA6: Molecular evolutionary genetics analysis version 6.0. *Mol Biol Evol.*
- 1036 2013;30(12):2725-9. doi: 10.1093/molbev/mst197.
- 1037 83. Livak KJ, Schmittgen TD. Analysis of relative gene expression data using real-time quantitative PCR and the $2^{-\Delta\Delta CT}$ method. *Methods.*
- 1038 2001;25(4):402-8. doi: 10.1006/meth.2001.1262.
- 1039
- 1040